

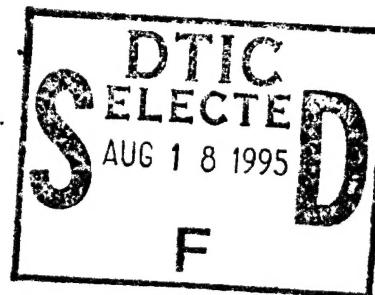
WL-TR-95-4009



**MODELING OF BIOMATERIALS FOR  
NON-LINEAR OPTICAL APPLICATIONS**

E. K. Karikari  
B. L. Farmer  
Department of Materials Science & Engineering  
University of Virginia  
Charlottesville, VA 22903

W. W. Adams  
R. Pachter  
Materials Directorate  
Wright Laboratory



January 1995

Interim Report for the Period January 01, 1993 - January 01, 1994

Approved for public release; distribution unlimited

Materials Directorate  
Wright Laboratory  
Air Force Materiel Command  
Wright-Patterson Air Force Base, OH 45433-7734

19950816 140

DTIC QUALITY INSPECTED 8

## NOTICE

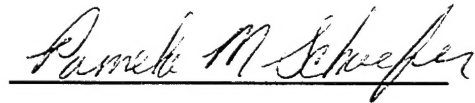
When Government drawings, specifications, or other data are used for any purpose other than in connection with a definitely Government-related procurement, the United States Government incurs no responsibility or any obligation whatsoever. The fact that the Government may have formulated or in any way supplied the said drawings, specifications, or other data, is not to be regarded by implication, or otherwise in any manner construed, as licensing the holder, or any other person or corporation; or as conveying any rights or permission to manufacture, use, or sell any patented invention that may in any way be related thereto.

This report is releasable to the National Technical Information Service (NTIS). At NTIS, it will be available to the general public, including foreign nations.

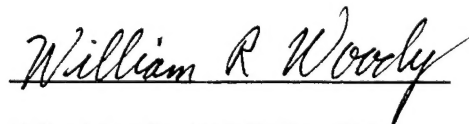
This technical report has been reviewed and is approved for publication.



W. WADE ADAMS  
Hardened Materials Technology Section  
Hardened Materials Branch



PAMELA SCHAEFER, Acting Chief  
Hardened Materials Branch  
Electromagnetic Materials and  
Survivability Division



WILLIAM R. WOODY, Chief  
Electromagnetic Materials and  
Survivability Division

If your address has changed, if you wish to be removed from our mailing list, or if the addressee is no longer employed by your organization please notify WL/MLPJ, Wright-Patterson AFB, OH 45433-7702 to help maintain a current mailing list.

Copies of this report should not be returned unless return is required by security considerations, contractual obligations, or notice on a specific document.

REPORT DOCUMENTATION PAGE			FORM APPROVED OMB NO. 0704-0188	
<small>Public reporting burden for this collection of information is estimated to average hour per response, including the time for reviewing instructions, searching existing data sources, gathering and maintaining the data needed, the complete and review the collection of information. Send comments regarding this burden estimate or any other aspects of this collection of information, including suggestions and reducing this burden to Washington Headquarters Services, Directorate for Information Operations and Reports, 1215 Jefferson Davis Highway, Suite 1204, Arlington, VA 22202-4302, and to the Office of Management and Budget, Paperwork Reduction Project (08704-0188, Washington, DC 20503.</small>				
1. AGENCY USE ONLY (Leave Blank)		2. REPORT DATE January 1995		3. REPORT TYPE AND DATES COVERED INTERIM 01/01/93-01/01/94
4. TITLE AND SUBTITLE MODELING OF BIOMATERIALS FOR NON-LINEAR OPTICAL APPLICATIONS			5. FUNDING NUMBERS  C F49620-90-C-9076 PE 62102 PR 2422 TA 04 WU 01	
6. AUTHOR(S) E.K. KARIKARI* B.L. FARMER* W.W. ADAMS**  R. PACHTER**				
7. PERFORMING ORGANIZATION NAME(S) AND ADDRESS(ES)  University of Virginia Department of Materials Science & Engineering Charlottesville, VA 22903			8. PERFORMING ORGANIZATION REPORT NUMBER	
9. SPONSORING MONITORING AGENCY NAME(S) AND ADDRESS(ES)  MATERIALS DIRECTORATE WRIGHT LABORATORY AIR FORCE MATERIEL COMMAND WRIGHT PATTERSON AFB OH 45433-7702			10. SPONSORING/MONITORING AGENCY REP NUMBER  WL-TR-95-4009	
11. SUPPLEMENTARY NOTES  *RDL Summer Faculty Program, University of Virginia, Dept. of Materials Science and Engineering **WL/MLPJ				
12a. DISTRIBUTION/AVAILABILITY STATEMENT  APPROVED FOR PUBLIC RELEASE; DISTRIBUTION IS UNLIMITED.			12b. DISTRIBUTION CODE	
13. ABSTRACT  Computational chemistry methods were used to explore the molecular conformations of a variety of optoelectronic biopolymers-spiropyran chromophore systems. An understanding of the molecular structure of such systems is required for the achievement of high $\chi(2)$ or $\chi(3)$ nonlinear optical (NLO) properties. Studies of the structures of such biologically-synthesizable materials that exhibit NLO response contribute insight and understanding needed for the invention of complex novel biomaterials having defined structures and controlled optical properties. The effects of spiropyran chromophore isomerization on poly-L-alanine having the peptide backbone in the $\alpha$ -helical or $\beta$ -sheet conformations were investigated. Two variations of the spiropyran chromophores on two copolymers, the hexapeptide poly(gly-ser-gly-ala-gly-ala) and the septipeptide poly(asp-arg-leu-ala-ser-tyr-leu) were also investigated. These polypeptides are compositionally representative of the naturally occurring amino acid sequences in silk and wool, having respectively, the $\beta$ -sheet and $\alpha$ -helical conformations. The structural possibilities for such materials could be very interesting. The helical or $\beta$ -sheet segments could be collinear, and the peptide-chromophore molecules able to order easily, perhaps into a liquid crystalline phase. Furthermore, the presence of the chromophore could prelude crystallization and stabilize the liquid crystalline phase. Upon irradiation with light, formation of the merocyanine could cause the $\alpha$ -helix segments to become non-collinear, thus disrupting the packing of the liquid crystalline phase. Not only would the material become colored, its opacity would also change as a result of disruption of the molecular packing.				
14. SUBJECT TERMS Computational chemistry, Non-linear optical properties, Biomaterials, Spiropyran, Poly-L-alanine, Chromophore			continued on back 15. NUMBER OF PAGES 63 16. PRICE CODE	
17. SECURITY CLASSIFICATION OF REPORT UNCLASSIFIED	18. SECURITY CLASS OF THIS PAGE. UNCLASSIFIED	19. SECURITY CLASS OF ABSTRACT UNCLASSIFIED	20. LIMITATION ABSTRACT UL	

### 13. ABSTRACT (contiued)

On the other hand, the packing of the polypeptide segments in the solid or liquid crystalline state may substantially alter the ability of the spiropyran to open and close, affecting its sensitivity to UV radiation and the kinetics of its color change. Results from molecular dynamics simulations show that the  $\alpha$ -helix and the  $\beta$ -sheet conformations of poly-L-alanine are destabilized by the open and closed forms of the chromophore, with the open form exerting a larger influence. The hydrogen bond which is formed between the oxygen (in the NO<sub>2</sub> group) in the merocyanine chromophore and the amide proton of the first alanine residue in the peptide chain stabilizes the  $\alpha$ -helix to some extent. The  $\beta$ -sheet structures achieve stability by forming intramolecular hydrogen bonds between the *i*th and (*i*+2)th, or *i*th and (*i*+3)th amino acid residues. The presence of the closed form of the chromophore forces the peptide chain in the  $\alpha$ -helical and  $\beta$ -sheet conformations into more compact structures as indicated by the smaller average end-to-end distance of the peptide chain. This effect is also demonstrated in the copolymer-spiropyran systems. The effect of the chromophore on the biopolymers chains is found to depend more on the starting conformation of the biopolymer than of the specific amino acid sequence.

Accession For	
NTIS CRA&I	<input checked="checked" type="checkbox"/>
DTIC TAB	<input type="checkbox"/>
Unannounced	<input type="checkbox"/>
Justification	
By	
Distribution /	
Availability Codes	
Dist	Avail and/or Special
A-1	

## TABLE OF CONTENTS

<u>SECTION</u>	<u>PAGE</u>
List of Figures	iv
List of Tables	vi
Foreword	vii
1. <u>INTRODUCTION</u>	1
1.1. Silk Biopolymers	6
1.2. Photochromic Biopolymers	10
2. <u>METHODS</u>	15
3. <u>RESULTS AND DISCUSSION</u>	20
3.1. Force Field	20
3.2. Energetics of the Spiropyran-Biopolymer Models	22
3.3. Molecular Dynamics Results	23
3.3.1. End-to-End Distance	25
3.3.2. Chromophore-Copolymer Systems	41
3.3.3. Variation in the $\phi$ and $\psi$ Dihedral Angles	43
3.4. Molecular Dynamics of Benzothiazolone-Spiro-Benzo- pyran-poly-L-alanine Systems	47
3.4.1. Variation in $\phi$ and $\psi$ Dihedral Angles	55
4. <u>CONCLUSIONS</u>	58
5. <u>FUTURE WORK</u>	60
6. <u>REFERENCES</u>	61

## LIST OF FIGURES

1. Closed and open forms of indoline spiropyran	2
2. Reversible photochromism in spiropyran	3
3. Benzothiazoline-spiro-benzopyran	4
4. $\beta$ -sheet conformation	8
5. $\alpha$ -helix	8
6. Absorption spectra of poly(L-glutamic acid) + 41 mol % spiropyran	11
7. Photochromic behavior of spiropyran-modified poly-L-glutamate	12
8. Model of pA[ $\alpha$ ]-M-pA[ $\alpha$ ]	13
9. Model of pA[ $\alpha$ ]	13
10. Model of pA[ $\beta$ ]-M-pA[ $\beta$ ]	14
11. Model of pA[ $\beta$ ]	14
12. Merocyanine showing bonds linking the two fragments	21
13. Torsional oscillations of the single bond in merocyanine	22
14. Temperature-time profile for pA[ $\alpha$ ]-M-pA[ $\alpha$ ]	26
15. Temperature-time profile for pA[ $\beta$ ]-M-pA[ $\beta$ ]	27
16. End-to-end distance as a function of time ( $\alpha$ -helix )	29
17. End-to-end distance as a function of time ( $\beta$ -sheet )	30
18. Number of H-bonds in $\alpha$ -helical structures (both chains) during simulation	33
19. Variation in distance of H-bond (O--H) in pA[ $\alpha$ ]-M-pA[ $\alpha$ ]	34
20. Conformation of alanine residues attached to the indoline and benzopyran groups of merocyanine	35
21. Number of H-bonds in $\beta$ -structures (both chains) during simulation	36
22. Molecular motions of pA[ $\alpha$ ]-M-pA[ $\alpha$ ]	38

23. Molecular motions of pA[ $\beta$ ]-M-pA[ $\beta$ ]	39
24. Molecular motions of (i) pA[ $\alpha$ ]-S-pA[ $\alpha$ ]; (ii) pA[ $\beta$ ]-M-pA[ $\beta$ ]; (iii) pA[ $\alpha$ ]	40
25. Average $\phi$ and $\psi$ dihedral angles of $\alpha$ -helical alanine residues	44
26. Average $\phi$ and $\psi$ dihedral angles of $\beta$ -alanine residues	45
27. $\phi$ vs $\psi$ variations in alanine residues 1,4, and 7 in pA[ $\alpha$ ]-M-pA[ $\alpha$ ]	46
28. End-to-end distance ( $\alpha$ -helix )	49
29. End-to-end distance ( $\beta$ -sheet )	50
30. Number of H-bonds in $\beta$ -structures during simulation	51
31. Molecular motions of pA[ $\alpha$ ]-BZM-pA[ $\alpha$ ]	52
32. Molecular motions of pA[ $\beta$ ]-BZS-pA[ $\beta$ ]	53
33. Molecular motions of (i) pA[ $\alpha$ ]-BZS-pA[ $\alpha$ ] ; (ii) pA[ $\beta$ ]-BZM-pA[ $\beta$ ]	54
34. Molecular conformation of ala1 of pA[ $\alpha$ ]	56
35. Molecular conformations of alanine residues attached to the thiazoline and benzopyran groups of pA[ $\alpha$ ]-BZM-pA[ $\alpha$ ]	57

## LIST OF TABLES

1. Internal coordinates and chain repeat distance for an $\alpha$ -helix	20
2. Internal coordinates and chain repeat distance for a $\beta$ -sheet	21
3. PE of indoline spiropyran-poly-L-alanine models	24
4. PE of benzothiazoline spiropyran-poly-L-alanine models	24
5. Statistical analysis of end-to-end distance of $\alpha$ -poly-L-alanine	28
6. Statistical analysis of end-to-end distance of $\beta$ -poly-L-alanine	31
7. Statistical analysis of end-to-end distance of Co-II( $\alpha$ )	41
8. Statistical analysis of end-to-end distance of Co-I( $\beta$ )	42
9. Average values of the internal coordinates in $\alpha$ -helical chain of poly-L-alanine-merocyanine system	43
10. Average values of the internal coordinates in $\beta$ -chain of poly-L-alanine-merocyanine system	43
11. Statistical analysis of end-to-end distance of $\alpha$ -poly-L-alanine attached to benzothiazoline spiropyran	47
12. Statistical analysis of end-to-end distance of $\beta$ -poly-L-alanine attached to benzoythiazoline spiropyran	47



## FOREWORD

The following report was prepared under the AFOSR RDL Summer Research Program under subcontract 93-102, F49620-90-C-9076. It was administered under the direction of the Materials Directorate, Wright Laboratory, Air Force Materiel Command, Wright Patterson Air Force Base, Ohio, with Dr. R.L. Crane as the Materials Directorate Project Scientist (WUD). This report covers the doctoral research (EKK) performed at the University of Virginia on computer simulations of NLO biopolymers.

EKK is very grateful for a doctoral fellowship from the University of Virginia Minority Programs (funded by the National Science Foundation).

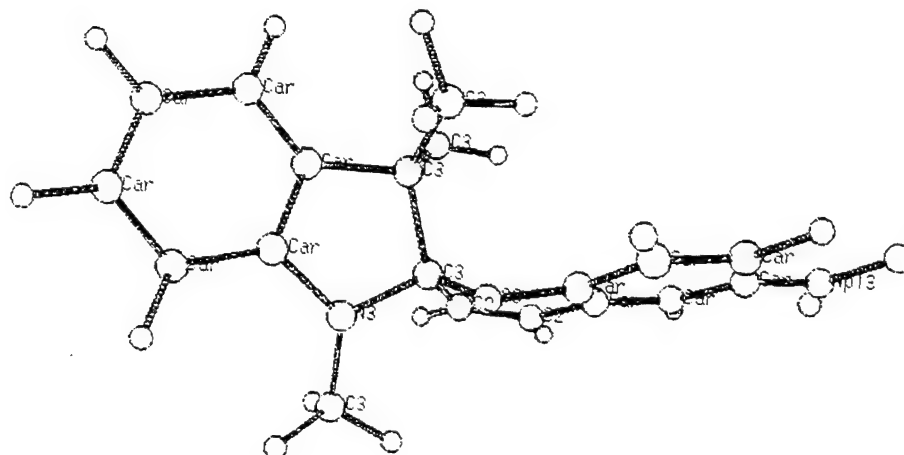
## Section 1

### INTRODUCTION

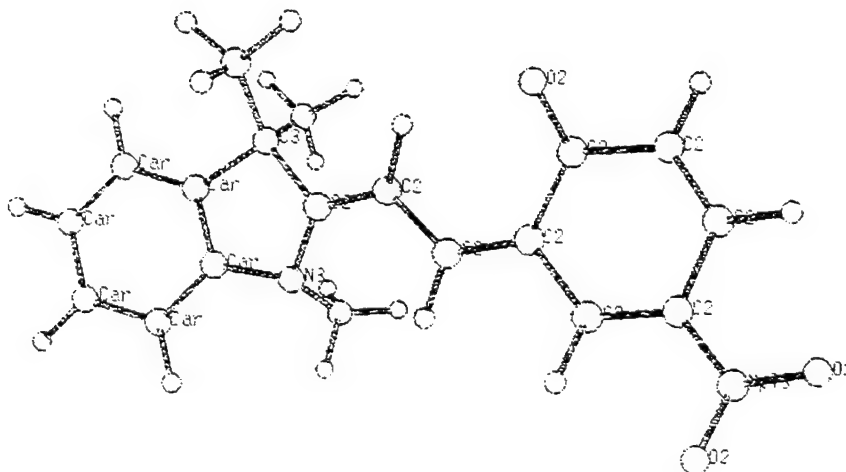
Photochromic biopolymers are polypeptides with substituent chromophores. These materials are being extensively investigated by the Air Force as potential nonlinear optical materials for laser hardening applications. Studies of the structures of biologically-synthesizable materials that may exhibit NLO response should contribute insight and understanding needed for the invention of complex biomaterials having defined structures and controlled optical properties. Helix-to-random coil transitions in polypeptides are induced by factors such as changes in solution polarity, temperature, and pH. Such transitions also occur when azo dyes and spiropyran chromophores are coupled to a polypeptide backbone ( 1 - 7 ). The polypeptide-chromophore systems are photoresponsive and consequently undergo changes in their peptide backbone conformation. This observation has spurred research interest in such photochromic-polypeptide systems as models for coupling photochemistry with backbone conformational changes. They are attractive systems because the peptide backbone can exist in definite ordered structures such as  $\alpha$ -helical or  $\beta$ -sheet conformations.

The chromophores investigated here are the spiropyrans ( Fig. 1 ). Current applications of the spiropyrans include high resolution photography, optical devices, variable transmission devices, photovoltaic and holographic systems ( 8 ). In the closed form, the indoline ( left ) and benzopyran ( right ) fragments of the spiropyran molecule are linked by a spiro carbon atom having tetrahedral  $sp^3$  hybridization. The two fragments are thus orthogonal to each other. Upon irradiation with light in the UV region of the electromagnetic spectrum,

spiropyrans undergo ring scission, converting from the colorless, closed form to a colored, open merocyanine form ( Fig. 2 ).



**(a ) closed form**



**(b) open form**

**Figure 1. Closed and open forms of indoline spiropyran**

Ring opening occurs by heterolytic dissociation of the bond between the spiro carbon and the pyran oxygen atoms, followed by molecular rearrangement. The central carbon atom becomes  $sp^2$  hybridized and the indoline and benzopyran moieties become coplanar. This facilitates delocalization of the  $\pi$  electrons between the indoline and benzopyran fragments, giving rise to an intense absorption band in the visible portion of the spectrum. Thermal energy or absorption of visible light causes the closed, spiropyran structure to re-form slowly.

Two variations of the spiropyran chromophore, the indoline and benzothiazoline derivatives (Fig.1 and Fig. 3 respectively) have been investigated. Steric factors would be considerably different in the benzothiazoline-based chromophore since it lacks the 3'-methyl substituents (9) present in the indoline spiropyran. (Divalent sulfur is substituted for the methylated in the five-member ring.)

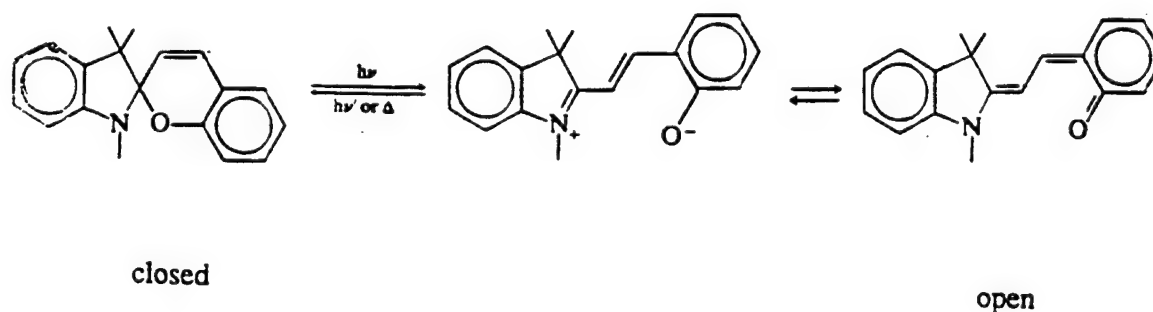


**Fig. 2. Reversible photochromism in spiropyran**

When the spiropyran is appended to a polypeptide, accumulation of charged merocyanine groups along the peptide chain can alter the chain conformation. This in turn influences the photochromic behavior of the spiropyran. Conformational calculations ( 7 ) on spiropyran-modified poly-L-glutamate show that the polypeptide chain conformation is perturbed by the open and closed forms of the chromophore, with the open form exerting a larger influence on the peptide chain.

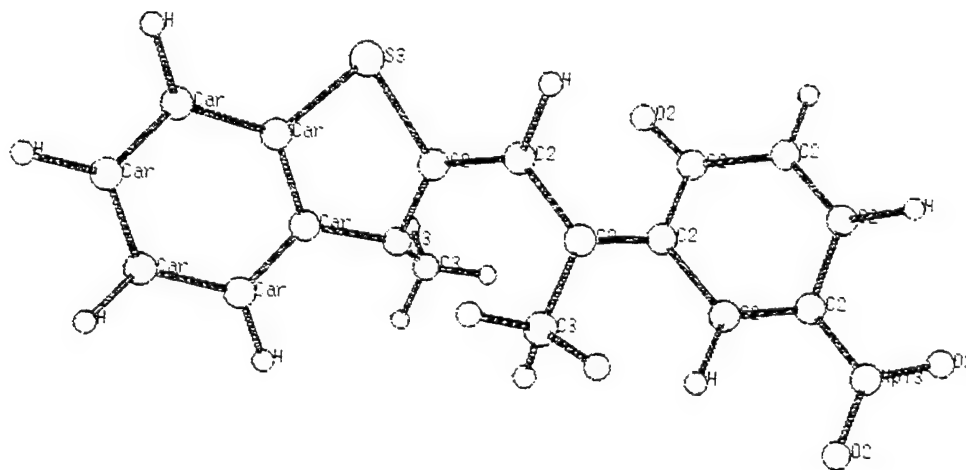


**Fig. 3. Benzothiazoline-spiro-benzopyran**

Various stable conformations exist in polypeptide backbones. These include the left-handed and right-handed  $\alpha$ -helices, the extended  $\beta$ -sheet, the PGI and PGII helices found in polyglycine, and PPI and PPII helices found in polyproline. The present molecular modeling calculations focused on polypeptide-spiropyran systems in which the polypeptide chain was initially in the  $\alpha$ -helical or  $\beta$ -conformation. Both homopolymer and copolymer chains have been considered. Poly-L-alanine, a homopolymer, in both the  $\alpha$ -helix and  $\beta$ -sheet conformations was studied in detail. Poly-L-alanine was chosen because it is the simplest

polypeptide found experimentally to adopt both the  $\alpha$ -helical and  $\beta$ -sheet conformations. Though the most stable conformation of an isolated poly-L-alanine molecule is the  $\alpha$ -helix, X-ray diffraction studies ( 10, 11 ) show that the molecule can also exist in an antiparallel or parallel  $\beta$ -sheet conformation in fibers mechanically stretched in steam or treated with suitable solvents.

The copolymers investigated were the hexapeptide poly(gly-ser-gly-ala-gly-ala), and the septipeptide poly(asp-arg-leu-ala-ser-tyr-leu). These polypeptides are compositionally representative of the naturally occurring amino acid sequences in silk and wool, having respectively, the  $\beta$ -sheet and  $\alpha$ -helical conformations.

Previous work ( 7 ) modeled the spiropyran-peptide system by attaching the spiropyran as a pendant side-group on the polymer. We have investigated the effects of alternate locations for the chromophore on the conformations of various polypeptides. For example, both open and closed forms were used as a blocking group at the amino terminus of the peptide. We also investigated systems in which two polypeptide chain segments were attached to the chromophore. The structural possibilities for such materials could be very interesting. The helical or  $\beta$ -sheet segments could be collinear, and the peptide-chromophore molecules able to order easily, perhaps into a liquid crystalline phase. Furthermore, the presence of the chromophore could preclude crystallization and stabilize the liquid crystalline phase. Upon irradiation with light, formation of the merocyanine could cause the  $\alpha$ -helix segments to become noncollinear, thus disrupting the packing of the liquid crystalline phase. Not only would the material become colored, its opacity would also change as a result of disruption of the molecular packing. On the other hand, the packing of the polypeptide segments may substantially alter the ability of the spiropyran to open and close, affecting its sensitivity to UV radiation and the kinetics of its color change.

### 1.1. Silk Biopolymers

Silk-like proteins have elicited scientific interest as they possess inherent properties which make them suitable for a variety of applications including high performance fibers ( 12 ), enzyme immobilization substrates ( 13 ), and polymers with highly controlled crystal morphologies ( 14 ). Silk produced by the species *Bombyx mori* is a fibrous material in which the protein portion is composed of fibroin ( consisting of crystalline fibers ), and a water-soluble component called sericin. Sericin contains a high percentage of polar amino acids, e.g. serine and aspartic acid, whereas the fibroin abounds in nonpolar amino acids, e.g. glycine and alanine. The silk fibroins have been investigated ( 15-27 ) in detail. The predominant conformation observed is the  $\beta$ -sheet conformation ( Figure 4 ), but other conformations, for example,  $\alpha$ -helical, polyglycine II, and collagen-like conformations are also found ( 15 ). The  $\beta$ -sheet conformation was also proposed ( 18, 19 ) for keratin in the hair which had been steam-stretched.

The antiparallel  $\beta$ -structures which consist of pleated  $\beta$ -sheets, can be divided into 4 main groups on the basis of their X-ray patterns ( 16, 17 ).

In group 1, the primary sequence of amino acids in *Bombyx mori* is Gly-Ala-Gly-Ala-Gly-[Ser-Gly(Ala-Gly)<sub>n</sub>]<sub>3</sub>-Ser-Gly-Ala-Ala-Gly-Tyr, where *n* is usually 2 or has an average value of 2. The characteristic X-ray pattern shows an axial period of 21 Å corresponding to the hexapeptide sequence Ser-Gly-Ala-Gly-Ala-Gly.

Group 2 fibroins are composed of alanine and glycine predominantly and probably have a repeating sequence of the type -[(Gly-Ala)<sub>x</sub>]<sub>n</sub>- where *x* = 4,5 or 6.

Group 3 fibroins are composed of long sequences of alanyl residues and feature an X-ray pattern similar to that of poly-L-alanine.

Group 4 fibroins consist of alanine and glutamic acid residues of the sequence  $[\text{Ala-Gln}]_n$ . Hydrolysis of glutamine in the intact protein yields glutamic acid.

In general,  $\beta$ -structures contain 20-45 % glycine, 20-50 % alanine, and 10-40 % serine. Thus, alternating copolymers of these amino acids might provide useful models for studying the structure of silk. Poly(L-Ala-Gly) is often used as the model for the crystalline fraction of *Bombyx mori* fibroin since the two crystalline forms of poly(L-Ala-Gly) are isomorphous with the two crystalline forms of silk.

In the  $\beta$ -conformation, the peptide chains form sheets with hydrogen-bonding between adjacent chains. The amino acid sidechains are accommodated between the sheets which are held together by van der Waals forces. The structural features are a chain repeat distance of  $\sim 7 \text{ \AA}$ , an interchain distance of  $\sim 4.7 \text{ \AA}$  in the direction of the hydrogen bond, and the N-H and C=O bonds nearly at right angles to the chain axis.

Figure 5 shows a right-handed  $\alpha$ -helical conformation. The  $\alpha$ -helical conformation in synthetic polypeptides was observed in the X-ray diffraction of poly( $\gamma$ -benzyl-L-glutamate) ( 20, 21 ). The characteristic structural features of the  $\alpha$ -helix are a pitch of  $5.4 \text{ \AA}$  and a residue translation of  $1.5 \text{ \AA}$ , approximating 18 residues in 5 turns. Hydrogen bonds are formed between the  $i^{\text{th}}$  and  $(i+4)^{\text{th}}$  amino acid residues.

Computational chemistry methods are essential tools for the analysis of the dynamics and structure of macromolecular systems, and also the theoretical prediction of the mechanical properties of such systems. Conformational energy calculations on representative polypeptide models have been used to study the structural characteristics of collagen ( 22, 23 ), poly(glycine) ( 24, 25 ), poly(alanine) ( 26, 27 ), poly(Ala-Gly) ( 27, 28 ), and poly(Glu) ( 27 ). Recently,



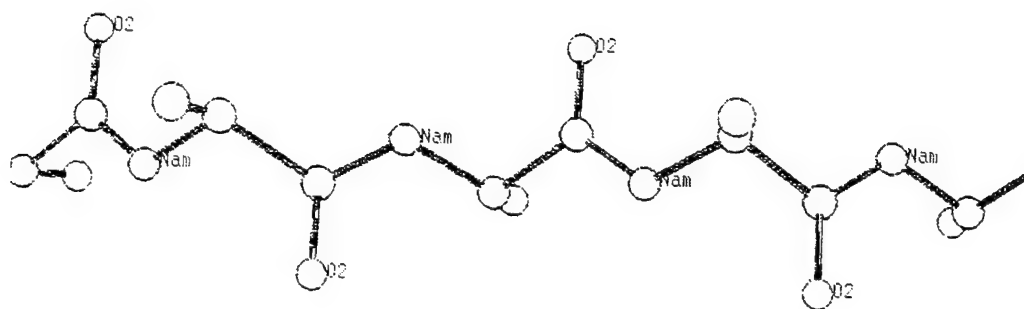


**Fig. 4.**  $\beta$ -sheet conformation

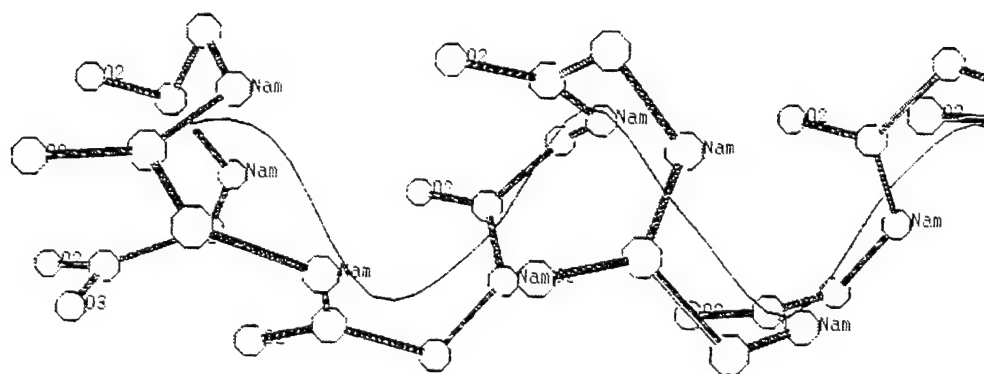


**Fig. 5.**  $\alpha$ -helix

Pachter et al. ( 27 ) used molecular simulations to predict the “spring-like” mechanical response of  $\alpha$ -helical poly(Ala) and poly(Glu) that have a reinforcing intramolecular hydrogen bonding network. Also investigated was poly(Gly-Ala) in the  $\beta$ -sheet conformation. For the sake of comparison, calculations were extended to include rigid-rod-like molecules containing an amide bond, i.e. poly(*para*-phenylene-terephthalamide) (PPTA). Results show that the silk fibers exhibit high compressive strength and as a result do not kink in compression. In contrast, high performance rigid-rod fibers, e.g. PPTA, demonstrate high tensile strength but low compressive strength ( 27 ), hence do kink in compression. The moduli calculated ( 27 ) for extended poly(Ala) and poly(Glu) chains were 160 GPa and 230 GPa respectively. The response of  $\alpha$ -helical poly(Ala) chains to strain revealed no kinking of the biopolymer in compression. A compressive modulus of 60 GPa was calculated. The results of this study show superior compressive mechanical properties of spider silk-type polypeptides over the known high performance rigid rod polymers.

Synthetic polypeptides, for example, poly( $\gamma$ -benzyl-L-glutamate), form lyotropic liquid crystals in solution. The supramolecular structure of concentrated polypeptide solutions resembles that of thermotropic, cholesteric liquid crystals (20). Above a certain concentration, the polypeptide solution separates into a birefringent phase composed of an anisotropic arrangement of the polypeptide molecules, and a dilute phase which under an optical microscope, exhibits a spherulitic structure typical of polymers crystallized from the bulk ( 21 ).

## 1.2. Photochromic Biopolymers

Photochromic biopolymers have been extensively investigated ( 1 - 7, 27, 28 ) as materials with unique nonlinear optical and mechanical properties. For example, when thin films of poly( $\gamma$ -benzyl-L-glutamate) are doped with a spiropyran chromophore, reversible changes occur in its optical rotatory power ( 3 ). Azo-modified poly-L-lysine shows a light-induced conformational change from an extended  $\beta$  chain to a random coil ( 4 ). A copolymer of  $\beta$ -benzyl-L-aspartate and  $\beta$ -(*m*-phenylazo)benzyl L-aspartate shows light-induced conformational changes from a left-hand to a right-hand helix ( 5 ). Photomodulation of conformation by sunlight in a spiropyran-attached poly-L-glutamic acid has been investigated ( 6 ).

Figure 6 shows the absorption spectra of poly(L-glutamic acid) containing 41 mol % of spiropyran in hexafluoro-2-propanol as a function of irradiation and dark adaptation time. The dark adapted polymer shows a broad absorption between 550-280 nm, with maxima occurring at 495, 370 and 312 nm. Upon irradiation or exposure to sunlight, the absorption in the visible region of the spectrum disappears. Circular Dichroism ( CD ) studies ( 6 ) show that the dark-adapted polymer exists as a random coil, and the chromophore is in its open form. During light-adaptation, the open form of the chromophore converts to the closed form, with a concurrent change in the peptide conformation from a random coil to an  $\alpha$ -helix. During dark-adaptation, a slow helix to coil dark reaction occurs and the chromophore converts to the colored, open form. A study of the kinetics ( 2 ) of the helix-to-coil dark reaction suggests a mechanism which involves helix $\rightarrow$ solvated helix $\rightarrow$ coil reactions. Conformational calculations ( 7 ) on spiropyran modified poly-L-glutamate (Fig. 7) show that the polypeptide chain conformation

is altered by the open and closed forms of the chromophore, with the open form exerting a larger influence on the peptide chain.

The stability of the open form could be influenced dramatically by the packing efficiency of the crystalline or liquid-crystalline state. Also, the site of attachment of the chromophore could influence the molecular rearrangements which occur during the open-close phenomenon.

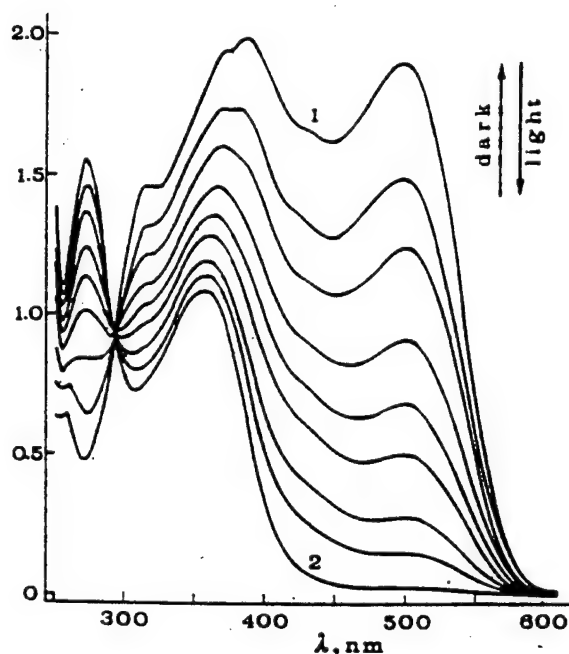


**Fig. 6. Absorption spectra of poly(L-glutamic acid)+41 mol% spiropyran.**  
(1, dark-adapted solution; 2, exposure to sunlight or irradiation). (6 )

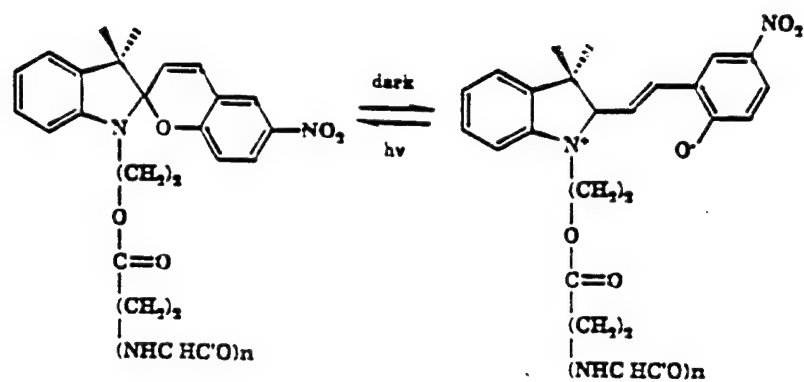


**Fig. 7. Photochromic behaviour of spiropyran-modified poly-L-glutamate**

Figure 8 shows two  $\alpha$ -helical poly-L-alanine chains attached to the open form of the spiropyran chromophore ( designated as  $\text{pA}[\alpha]\text{-M-pA}[\alpha]$  ), while Figure 9 depicts the biopolymer without the spiropyran chromophore (designated as  $\text{pA}[\alpha]$  ). Figure 10 shows two  $\beta$ -poly-L-alanine chains attached to the open form of the spiropyran chromophore ( designated as  $\text{pA}[\beta]\text{-M-pA}[\beta]$  ), while Figure 11 shows the unsubstituted poly-L-alanine ( designated as  $\text{pA}[\beta]$  ).

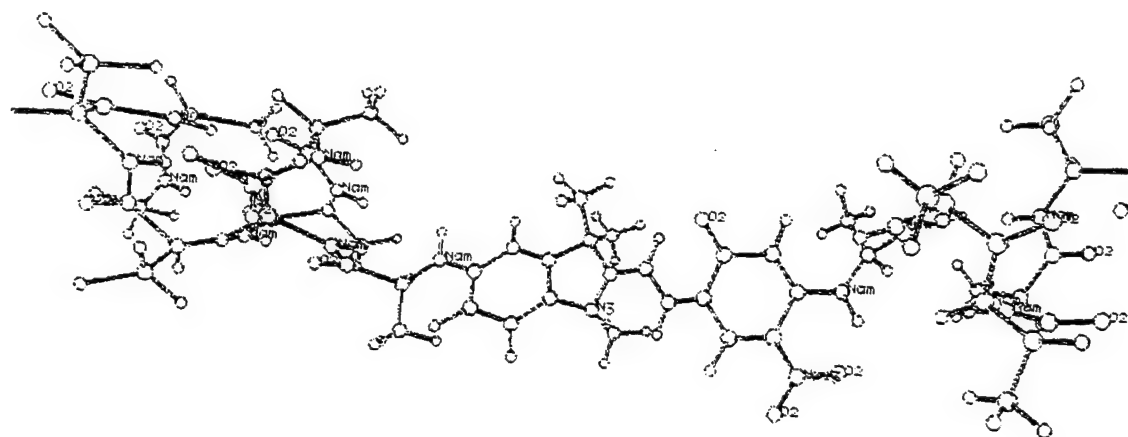


Fig. 8. Model of pA[ $\alpha$ ]-M-pA[ $\alpha$ ]

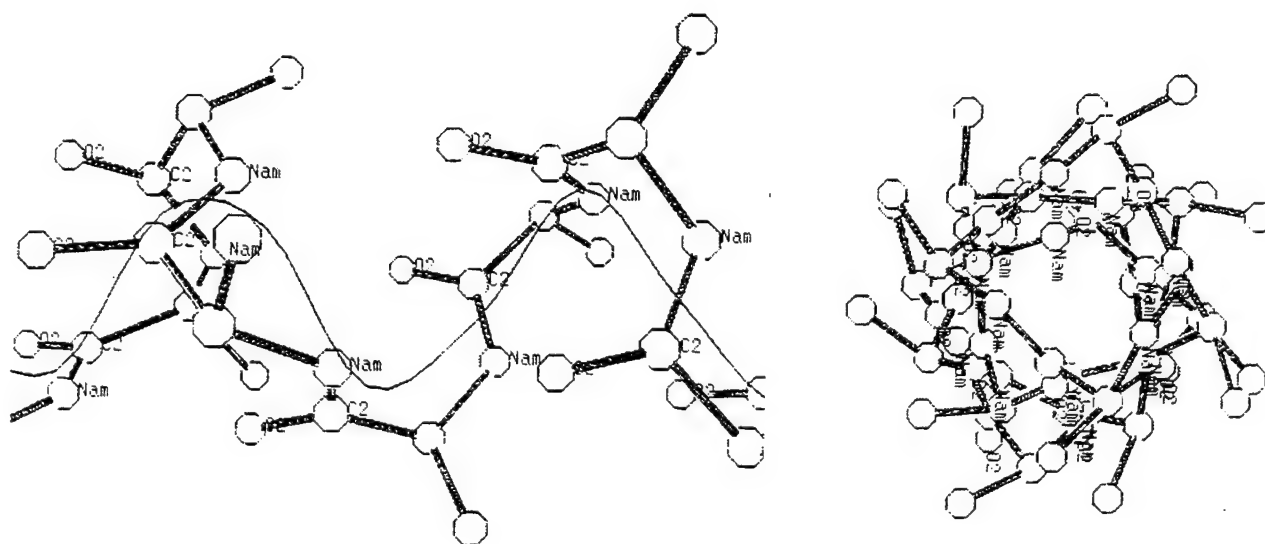


Fig. 9. Model of pA[ $\alpha$ ]. On the right is shown the view along the chain axis.

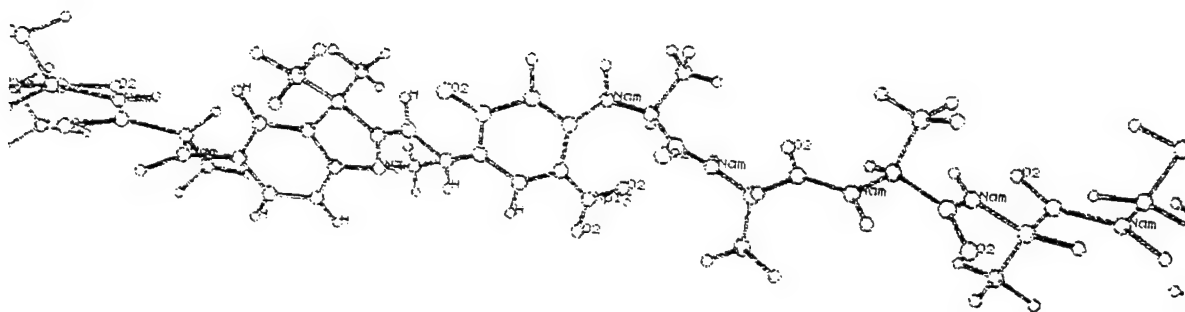


Fig. 10. Model of pA [β]-M-pA [β]

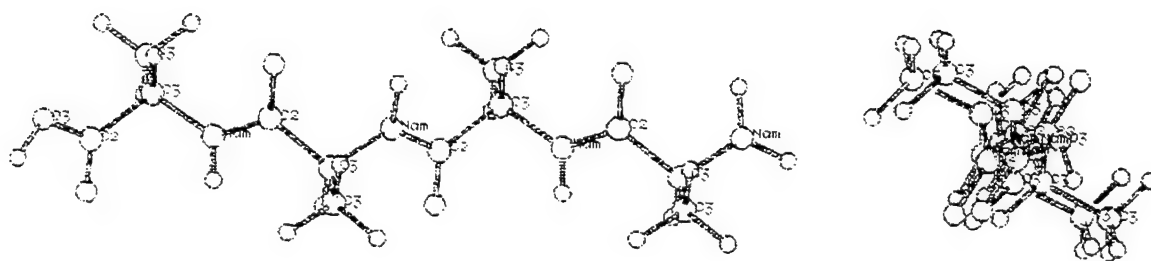


Fig. 11. Model of pA [β]. On the right is shown the view along the chain axis.

## Section 2

### METHODS

Modeling calculations were made using the SYBYL Molecular Modeling Software package ( version 6.01 ) ( 29 ).

Molecular mechanics ( MM ) was used to generate and evaluate conformations of chromophore-polypeptide molecules. Molecular dynamics ( MD ) was used to evaluate the effect of a chromophore on the conformational properties of the polypeptide and to address the issue of molecular flexibility in the system.

MM and MD calculations are based on a classical description of the bonding in a molecular system. Bond lengths, bond angles, torsion angles, non-bonded interactions, and electrostatic interactions are described in terms of force constants derived from a large body of vibrational and crystallographic data ( 30 ). Each cycle of energy minimization can be thought of as a step in conformational space. The MM approach is primarily concerned with geometrical optimization of molecular conformations by finding the structural geometry that results in the lowest total potential energy ( 31, 32 ). The total potential energy of the molecule is the summation of the contributions by individual potential functions.

$$PE = \Sigma E_{\text{stretch}} + \Sigma E_{\text{bend}} + \Sigma E_{\text{torsion}} + \Sigma E_{\text{vdw}} + \Sigma E_{\text{elec}} \quad (1)$$

where

$E_{\text{stretch}}$  = bond stretching energy term

$E_{\text{bend}}$  = angle bending energy term

$E_{\text{torsion}}$  = torsional energy term



$E_{vdw}$  = van der Waals energy term ( Leonard Jones nonbonded potential )

$E_{elec}$  = electrostatic energy term.

The relevant equations for each of these energy terms are as given below:

$$E_{stretch} = 1/2k_i^s(l_i - l_o)^2 \quad ( 2 )$$

where  $k_i^s$  is the bond stretching force constant in kcal/mol-Å<sup>2</sup>

$l_i$  is the length of the ith bond

$l_o$  is the equilibrium length of the ith bond

$$E_{bend} = 1/2k_i^b(\theta_i - \theta_i^o)^2 \quad ( 3 )$$

where  $k_i^b$  is the angle bending force constant in kcal/mol-deg<sup>2</sup>

$\theta_i$  is the angle between two adjacent atoms

$\theta_i^o$  is the equilibrium value for the ith angle

$$E_{torsion} = 1/2k_i^t(1 + s/|s| (\cos\phi |s|) ) \quad ( 4 )$$

where  $k_i^t$  is the torsional barrier in kcal/mol

$s$  is the eclipsed/staggered rotational degeneracy constant

$$E_{vdw} = k_{ij}^{nb}(1/a_{ij}^{12} - 2/a_{ij}^6) \quad ( 5 )$$

where  $k_{ij}^{nb}$  is the van der Waals constant in kcal/mol

$a_{ij} = r_{ij}/(r_i + r_j)$ ,  $r_i$  is the van der Waals radius of atom i (Å)

$r_{ij}$  = the distance between atoms i and j

$$E_{\text{elec}} = 332.17 \sum_{i=1}^{N_{\text{atoms}}} \sum_{j>i} Q_i Q_j / D_{ij} r_{ij} \quad (6)$$

where  $D_{ij}$  = the value of the dielectric function for atoms  $i$  and  $j$

$Q_i$  = the net atomic charge at atom  $i$  (  $e^-$  )

$r_{ij}$  = the distance between atoms  $i$  and  $j$  (  $\text{\AA}$  )

The SYBYL/BIOPOLYMER module was used to model the peptide chain conformations to be attached to the indoline and benzopyran components of the spiropyran chromophore. The biopolymer modeling uses the concept of a monomer and builds and modifies structures on a residue by residue basis. The polypeptides were modeled as  $\alpha$ -helices or  $\beta$ -sheets consisting of 7 amino acid residues. It has been reported ( 33 ) that the minimum peptide main-chain length for  $\alpha$ -helix formation corresponds to 7 amino acid residues. The C-terminus was blocked by an N-methyl amide ( $-\text{HNCH}_3$ ) group, while the chromophore was used as a blocking group at the N-terminus of the peptide.

The conformational calculations on polypeptides took into account electrostatic interactions. These were calculated by a partial charge method ( the Del Re method ) which employs the concept of localized bond orbitals. The Tripos force field treats hydrogen bonds as non-directional and electrostatic in nature. During calculations, hydrogen bond energies are accounted for by scaling the van der Waals radius between the hydrogen bond acceptors ( N, O ) and hydrogens bonded to hydrogen bond donors ( N, O ). Structures were minimized using MAXIMIN2 which is a full-relaxation energy minimization scheme provided in SYBYL. The default minimization procedure ( Powell method ) was used. This is an iterative method in which the atomic coordinates are modified from one iteration to the next in order to lower the energy of the structure. The

method is similar to the conjugate gradient method, but uses more advanced rules to determine the descent direction.

MD is an extension of the molecular mechanics method of conformational analysis, employing the same semiempirical potential functions and associated force field to evaluate atomic interactions. MD calculations incorporate kinetic (i.e. thermal ) energy to provide a dynamic view of the system as a function of time and/or temperature. The atomic positions and velocities are iteratively computed in femtosecond ( fs ) time steps to provide a description of the natural molecular motions available to the system at the prescribed temperature. In simple terms, the MD calculations proceed as follows. First the force acting on each atom is computed ( from the derivative of the potential energy ) for all the interactions (bond stretches, bond angles, torsions, van der Waals and electrostatic) in the system. Subsequent numerical integration of classical Newtonian equations of motion (  $F = ma$ ,  $v = at$  ) using the Verlet ( or Leapfrog ) method ( 34 ) yields the individual atomic velocities and new atomic positions. In the Verlet method, the velocity is calculated at odd half integral multiples of  $\Delta t$ , while the position is calculated at integral multiples of  $\Delta t$ . The velocities of the atoms are then scaled at each time step to the specified temperature of the simulation using the equation:

$$3Nk_B T = \sum m_i v_i^2 \quad (7)$$

where  $T$  is the absolute temperature,  $k_B$  is Boltzman's constant,  $m_i$  and  $v_i$  are the mass and velocity of the  $i^{\text{th}}$  atom, and  $N$  is the total number of atoms. After one time step ( 1 fs ) these scaled velocities bring the atoms to new positions and modify the forces they experience. The forces are once again evaluated and the procedure is repeated until the simulation accumulates a specified number of time steps. A detailed description of MD is given by McCammon ( 35 ).

MD was used to simulate the natural molecular motions of the chromophore-bound polypeptides at 300 K. Initially the system was heated from 0 K to the target temperature of 300 K in 50 K increments. The total simulation time employed was 62,000 fs including 10,000 fs each of heating and equilibration stages of the computation. The time step used for each simulation was 1 fs. Atomic positions and velocities were stored and data analysis was carried out by considering data at 50 fs intervals. Momenta were reset and nonbonded interaction lists were updated every 25 fs. The nonbonded cutoff distance was 8.0 Å. The temperature coupling factor, a parameter used to impose gradual temperature changes, was 10. All atoms were included explicitly in the simulation. The simulation was carried out without solvent, representing the molecule as it might exist and behave *in vacuo*.

The Tripos force field in SYBYL version 6.01 was used in the molecular mechanics and molecular dynamics calculations. The force field has been shown ( 29 ) to produce molecular geometries close to the crystal structures of a variety of organic molecules and biopolymers. Calculations using the Tripos force field were found ( 29 ) to compare well with the Amber force field, developed primarily for biopolymer calculations.

## Section 3

### RESULTS AND DISCUSSION

#### 3.1. Force Field

Obtaining realistic results requires success on two distinct levels: completeness of the model and the accuracy of the force field description. The Tripos Force field and its associated potential energy functions were unmodified. To test the reliability of the Tripos force field in biomolecular modeling, unsubstituted models of poly-L-alanine in the  $\alpha$ -helical and  $\beta$ -sheet conformations were built and minimized using the Tripos and the Kollman-All-Atom force fields. The results from each were then compared with experimental values obtained from X-ray diffraction ( 18, 19, 21 ). Tables 1 and 2 show a comparison of the results from the force field methods with X-ray diffraction. The tables show that the Tripos force field is suitable for biopolymer modeling

Although this force field is parameterized for use with organic molecules and biopolymer molecules, its applicability to the spiropyran molecule, especially

Table 1. Internal coordinates and chain repeat distance for an  $\alpha$ -helix

	X-ray	Tripos	Kollman
$\phi$ (deg)	-58.0	-59.9	-57.6
$\psi$ (deg)	-47.0	-44.5	-47.1
$c$ (Å)	27.0	27.2	27.1

Table 2. Internal coordinates and repeat distance for an isolated  $\beta$ -sheet

	<b>X-ray</b>	<b>Tripes</b>	<b>Kollman</b>
$\phi$ (deg)	<b>-139.0</b>	<b>-140.8</b>	<b>-145.8</b>
$\psi$ (deg)	<b>139.0</b>	<b>139.4</b>	<b>145.0</b>
$c$ (Å)	<b>7.0</b>	<b>7.0</b>	<b>6.9</b>

the merocyanine is questionable. The alternating bond sequence ( double-single-double bonds ) (Figure 12 ) linking the two fragments of the merocyanine, has substantial electron delocalization. All these bonds have character intermediate between single and double bonds. and can potentially change with the conformation. The Tripes force field describes these bonds as immutably single or double; hence the use of the unmodified force field may cause unrealistic rigidity in this part of the molecule. Figure 13 shows the torsional oscillations of the single bond in merocyanine-substituted poly-L-alanine. The excursions from the trans conformation are limited (  $\pm 10^\circ$  ) but still considerably larger (  $\pm 5^\circ$  ) than observed for the double bonds. Over longer simulation times, conformational transitions to gauche values would be expected. Since the behavior of the chromophore may not be representative, this analysis will focus on the behavior of the peptide chains.

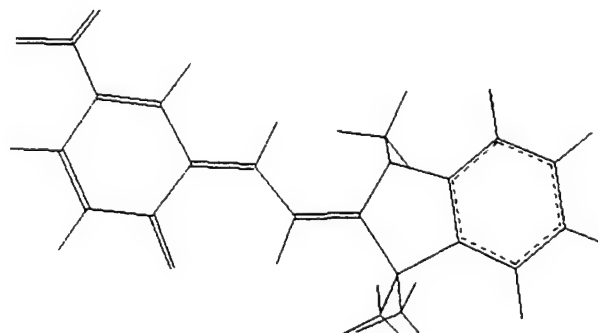


Fig. 12. Merocyanine, showing bonds linking the two fragments

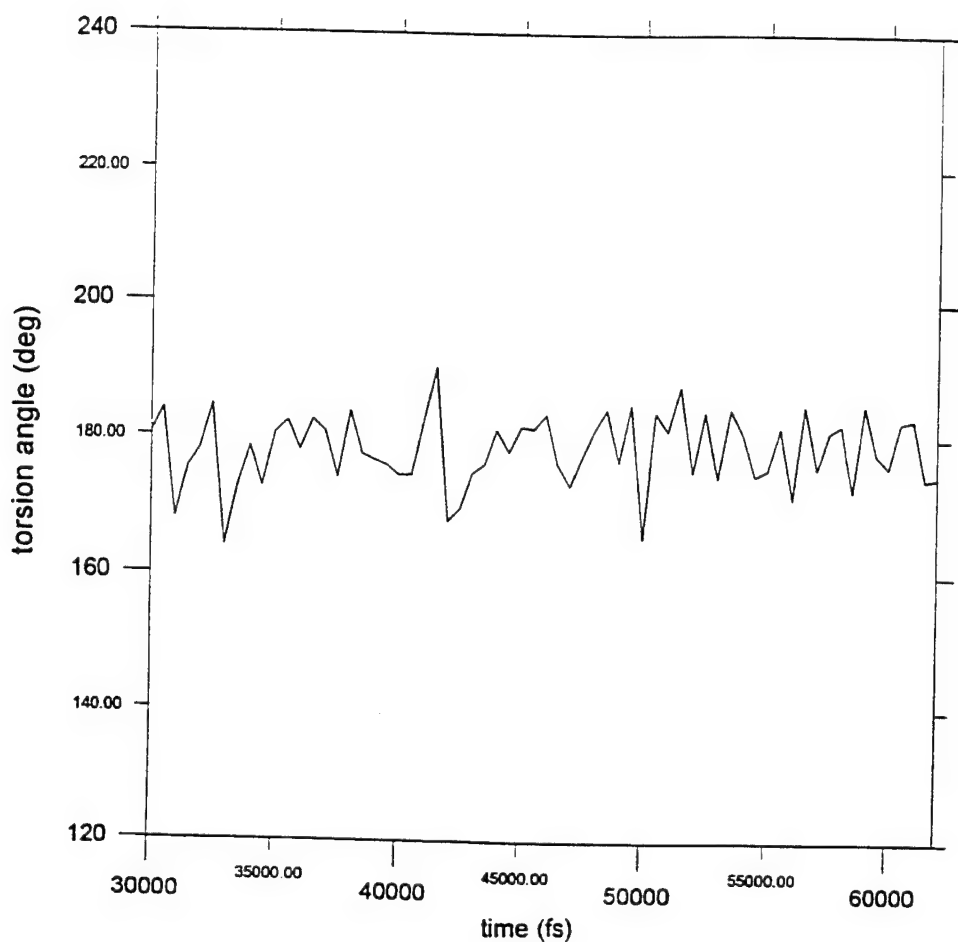


Fig. 13. Torsional oscillations of the single bond in merocyanine

### 3.2. Energetics of the Spiropyran-Biopolymer Models

Table 3 shows the potential energies for the indoline spiropyran-poly-L-alanine systems with the peptide backbone in the helical or beta sheet conformation. Also included in the table are the energies of closed and open forms of spiropyran, and unsubstituted poly-L-alanine in  $\alpha$ -helical and  $\beta$ -sheet conformations, and having a total length comparable to that of each of the biopolymer-chromophore systems. The large difference in energy between the

unsubstituted  $\alpha$ -helical and  $\beta$ -poly-L-alanine is due to the fact that the calculations were made for an isolated chain of  $\beta$ -poly-L-alanine in which the stabilization effect of intermolecular hydrogen bonding is absent. It should be pointed out that a gain in stabilization energy ( comparable to that of the helix ) of the  $\beta$ -conformation is normally achieved through intermolecular hydrogen bonding between stacked parallel or antiparallel sheets. Table 4 shows a similar calculation for the biopolymer coupled to benzothiazoline-spiro-benzopyran.

The sum of the energies of the isolated molecules of poly-L-alanine and the indoline spiropyran is  $\sim 49$  kcal/mol, while the energy of the bonded pA[ $\alpha$ ]-S-pA[ $\alpha$ ] or pA[ $\alpha$ ]-M-pA[ $\alpha$ ] is 65 kcal/mol. Thus, upon derivatizing  $\alpha$ -helical poly-L-alanine with the chromophore, there is a significant increase in the energy of the system of about 16 and 32 kcal/mol for the spiropyran- and merocyanine-substituted poly-L-alanine systems respectively. The increase in energy results from some interference between the helix and the chromophore. The energy increase upon incorporating the chromophore into the  $\beta$ -poly-L-alanine chain is less than observed for the helix.

For the benzothiazline spiropyran-poly-L-alanine systems, an energy increase of  $\sim 30$  kcal/mol results upon attaching the chromophore to  $\alpha$ -helical and  $\beta$ -poly-L-alanine chains. The minimum energy conformation is the  $\alpha$ -helical poly-L-alanine-chromophore system irrespective of the form of the chromophore.

### 3.3. Molecular Dynamics Results

Molecular dynamics is used to examine molecular flexibility in the biopolymer-chromophore systems, and the effect of mode of attachment of the peptide chains on the stability of the closed and open forms of the chromophore.



Table 3. PE ( in kcal/mol ) of indoline spiropyran-poly-L-alanine models

Polypeptide-chromophore system	E kcal/mol
pA[ $\alpha$ ]-S-pA[ $\alpha$ ]	65
pA[ $\alpha$ ]-M-pA[ $\alpha$ ]	80
pA[ $\beta$ ]-S-pA[ $\beta$ ]	92
pA[ $\beta$ ]-M-pA[ $\beta$ ]	103
pA[ $\alpha$ ]	32
pA[ $\beta$ ]	74
S	16
M	17

Table 4. PE ( in kcal/mol ) of benzothiazoline spiropyran-poly-L-alanine models.

Polypeptide-chromophore system	E kcal/mol
pA[ $\alpha$ ]-BZS-pA[ $\alpha$ ]	82
pA[ $\alpha$ ]-BZM-pA[ $\alpha$ ]	86
pA[ $\beta$ ]-BZS-pA[ $\beta$ ]	88
pA[ $\beta$ ]-BZM-pA[ $\beta$ ]	112
pA[ $\alpha$ ]	32
pA[ $\beta$ ]	74
S	23
M	17

The variation in the end-to-end distance of the chains attached to the chromophores was studied, as well as the angular variation in the internal coordinates (  $\phi$  and  $\psi$  dihedral angles ) which define the structure of the peptide. The  $\phi$  and  $\psi$  dihedral angles measure the torsions about the rotationally permissive bonds in the backbone of the amino acid residues, and hence, are the most important coordinates in determining the peptide chain conformation. For a peptide chain in the  $\alpha$ -helical conformation, the values of the  $\phi$  and  $\psi$  dihedral angles are  $-58^\circ$  and  $-47^\circ$ , respectively, while for the  $\beta$ -sheet the values are  $-139^\circ$  and  $135^\circ$ . Molecular dynamics simulations were carried out at 300 K for a period of 42,000 fs, after 10,000 fs each of heating and equilibration. Shown in Figures 14 and 15 are the temperature-time profiles during the MD simulation for the  $\alpha$ -helical or  $\beta$ -poly-L-alanine-chromophore systems investigated.

### 3.3.1. End-to-End Distance

The extent of motion that occurred during the molecular dynamics simulation was observed by plotting the end-to-end distance ( between the amide nitrogen of residue 1 and the carbonyl carbon of residue 7 of the chain attached to the indoline group of the chromophore ) as a function of simulation time. Tables 5 and 6 show the statistical analysis of the end-to-end distance of the  $\alpha$ -helical and  $\beta$ -chains of poly-L-alanine derivatized with the open and closed forms of indoline spiropyran, and the unsubstituted poly-L-alanine in either  $\alpha$ - or  $\beta$ -conformation. The standard deviation gives a measure of the flexibility of the system, while the average distance measures the degree to which the biopolymer chain is extended or coiled. The values listed on the left are for the peptide attached to the indoline

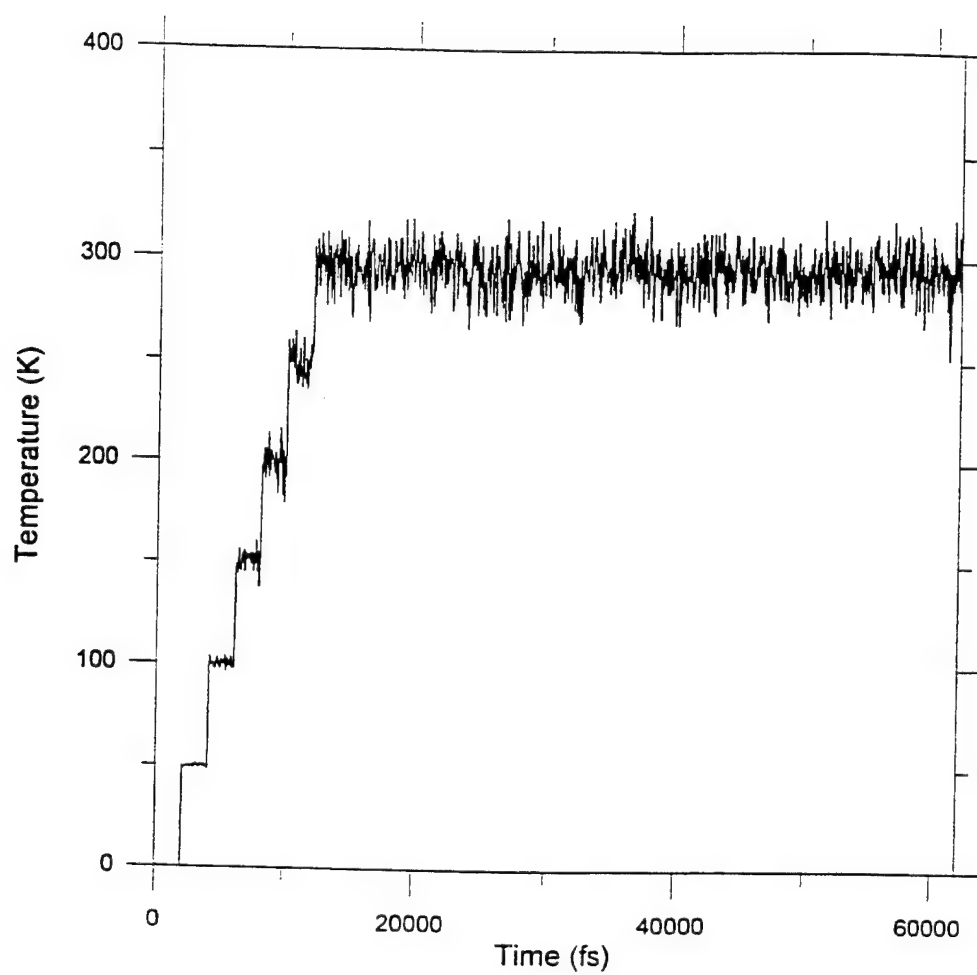


Fig. 14. Temperature-time profile for pA[α]-M-pA[α]

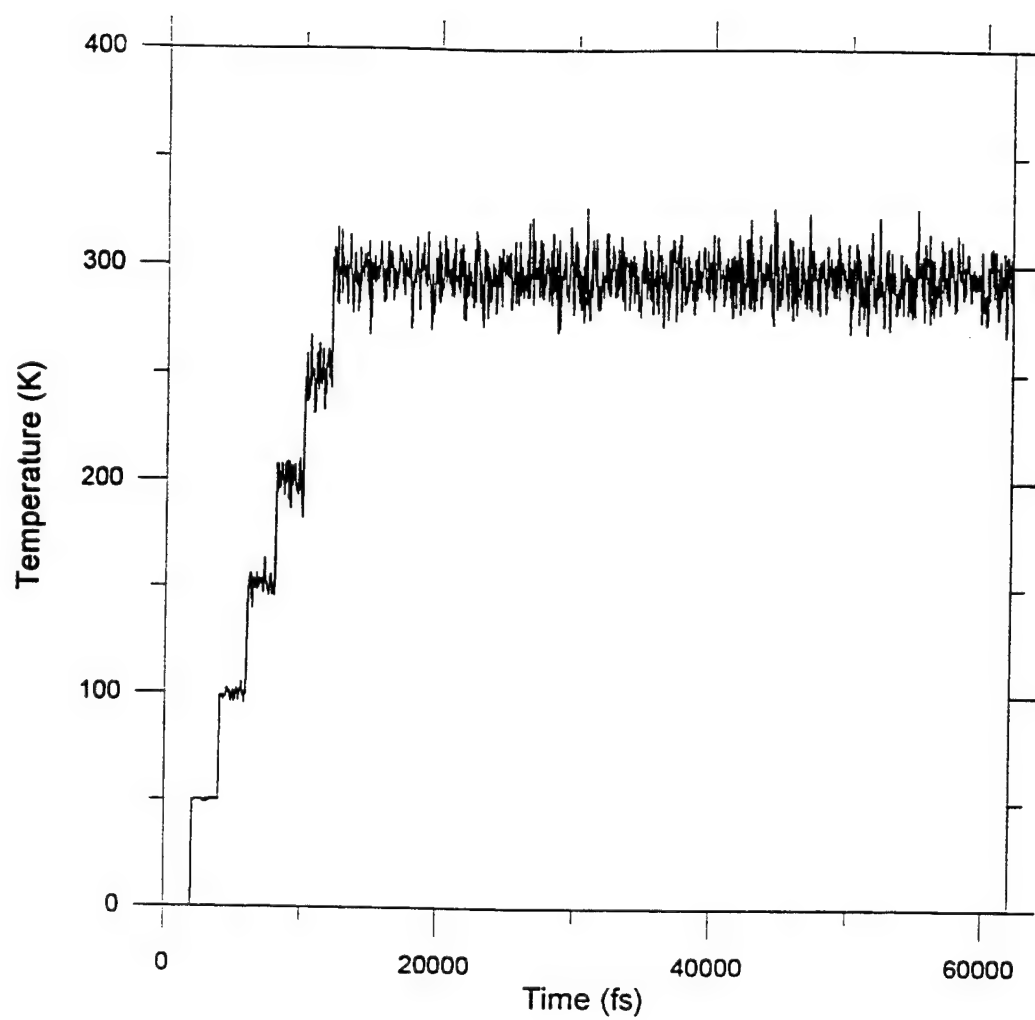


Fig. 15. Temperature-time profile for pA[β]-M-pA[β]

group, while those on the right are for the benzopyran group

Calculations for the unsubstituted poly-L-alanine are made for a model composed of 20 alanine residues. The N-terminus of the chain was blocked by an N-acetyl group and the C-terminus by N-methyl amide. The first 7 ( of the 20 ) alanine residues in the resulting model were used to determine the end-to-end distance values in the table. In the chromophore-biopolymer systems, the N-terminus of one chain was blocked by the chromophore and the C-terminus by an N-methyl amide group. This blocking could influence the stability of the chain. The stability of the unsubstituted biopolymer is gained from the intramolecular  $i^{\text{th}}-(i+4)^{\text{th}}$  hydrogen bonds between the alanine residues. Shown in Figures 16 and 17 are plots of end-to-end distance for the indoline spiropyran attached to  $\alpha$ -poly-L-alanine and  $\beta$ -poly-L-alanine respectively. Also included in the plots are the data for the unsubstituted  $\alpha$ -helical and  $\beta$ -poly-L-alanine.

Table 5. Statistical analysis of end-to-end distance of  $\alpha$ -poly-L-alanine

initial length of helix = 11 Å

	pA[ $\alpha$ ]-M-pA[ $\alpha$ ]	pA[ $\alpha$ ]-S-pA[ $\alpha$ ]	pA[ $\alpha$ ]
average (Å)	12.7, 11.2	8.1, 11.9	8.0
Std deviation (Å)	2.7, 2.3	1.5, 2.0	1.2

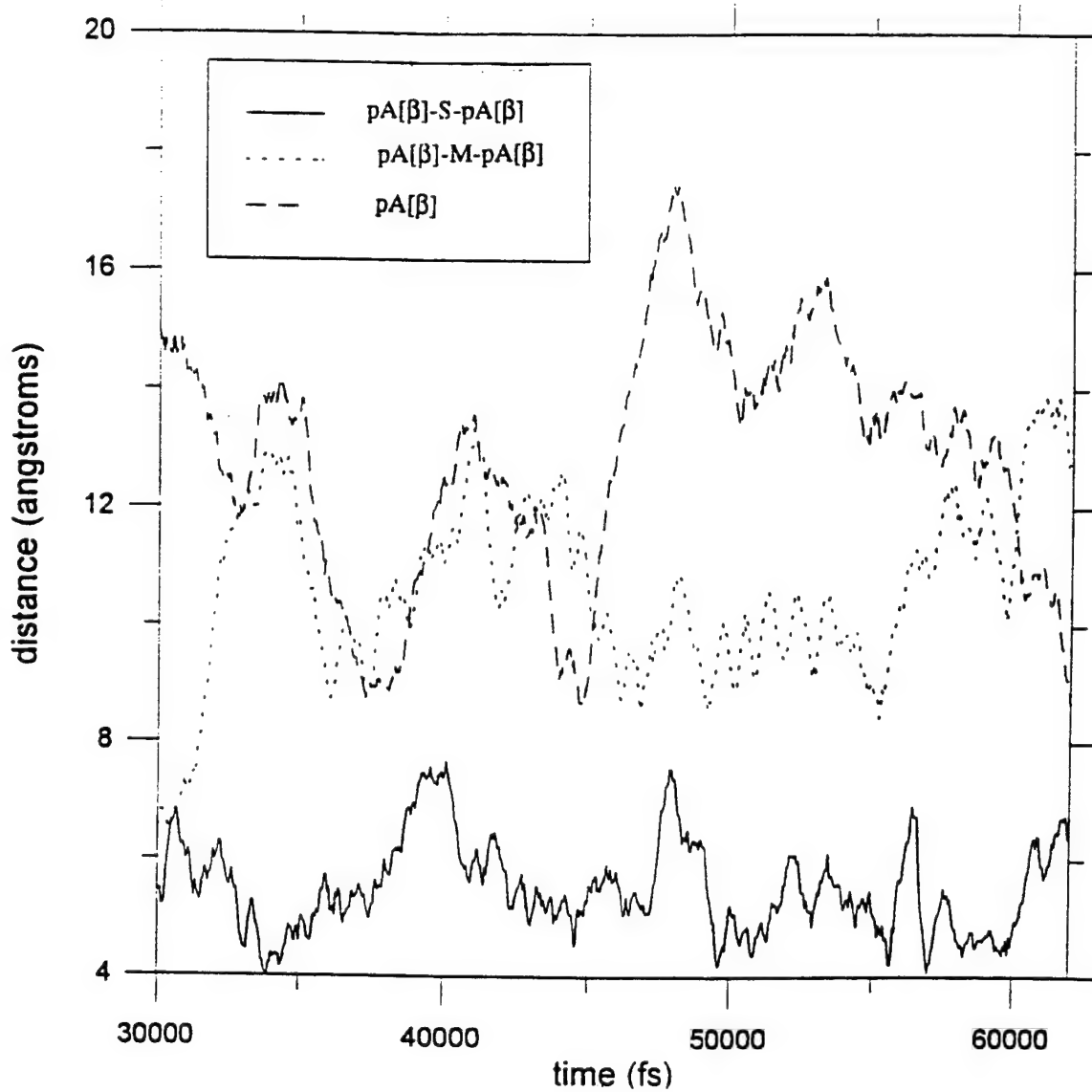


Fig. 16. End-to-end distance as a function of time (  $\alpha$ -helix )

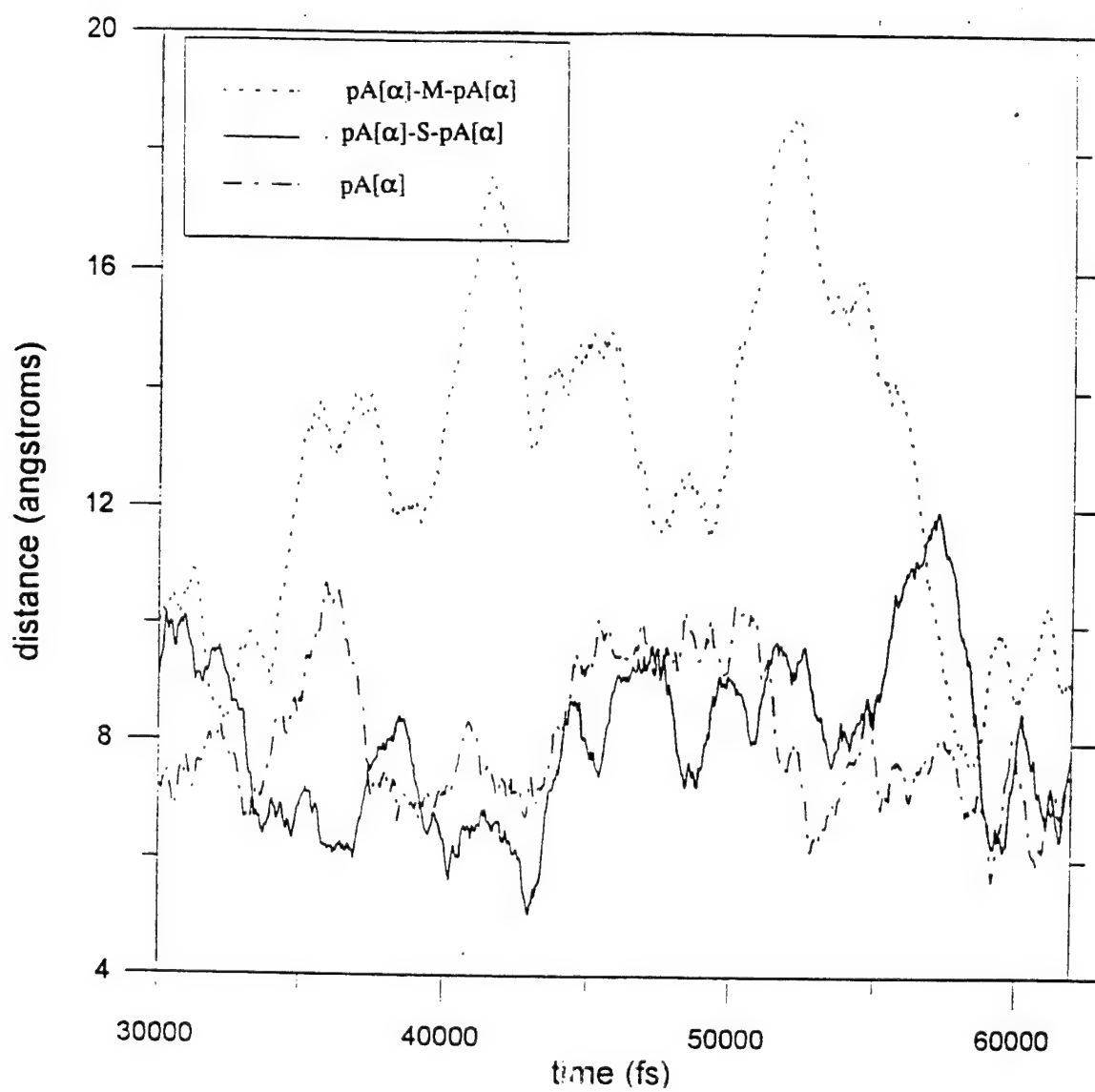


Fig. 17. End-to-end distance as a function of time (  $\beta$ -sheet )

Table 6. Statistical analysis of end-to-end distance of  $\beta$ -poly-L-alanine

initial length of  $\beta$ -chain = 24.0 Å

	pA[ $\beta$ ]-M-pA[ $\beta$ ]	pA[ $\beta$ ]-S-pA[ $\beta$ ]	pA[ $\beta$ ]
average (Å)	10.6, 11.5	5.5, 7.3	12.8
Std deviation (Å)	3.0, 2.4	2.7, 1.9	2.0

Results show that there is a significant deviation in the end-to-end distance of both  $\alpha$ - and  $\beta$ -poly-L-alanine chains in the presence of the chromophore. The average length of the  $\alpha$ -helical chain attached to the merocyanine during the simulation is slightly higher (  $\sim 2$  Å ) than the starting value of the helix and 3-4 Å longer than the poly-L-alanine without a chromophore. This indicates that the helix tends to uncoil and extend during the simulation, while the unsubstituted helix tends to coil up.

Conversely, the extended  $\beta$ -chain, having an initial length of  $\sim 24$  Å, assumes a more compact structure during the dynamics. For example, the merocyanine-substituted biopolymer shows a contraction of the chains during the dynamics, resulting in an average distance of  $\sim 11$  Å, a value close to the initial value of an  $\alpha$ -helix. Substitution causes more collapse of the  $\beta$ -sheet than was observed in poly-L-alanine by itself. Compared to the merocyanine, the spiropyran forces the peptide chain, initially in either the  $\alpha$ -helical or  $\beta$ -sheet conformation, into more compact structures as indicated by the lower average distance.



Figure 16 shows that the presence of the merocyanine causes the  $\alpha$ -helical biopolymer backbone to uncoil and extend. The spiropyran does not have much effect. The number of hydrogen bonds in the  $\alpha$ -helical poly-L-alanine chain is shown in Figure 18. The number of hydrogen bonds decreases from the initial ( $t=0$ ) value of 8. This allows the biopolymer chain to uncoil and extend.

The MD simulation shows that a hydrogen bond is formed between the oxygen in the  $\text{NO}_2$  group on the merocyanine chromophore and the amide hydrogen of the first alanine residue in the peptide chain. This hydrogen bond remains intact during the dynamics simulation (as seen in Figure 19), although the length varies slightly from an initial ( $t=0$ ) value of  $1.8 \text{ \AA}$  ( before the heating cycle of the dynamics ). The hydrogen bond stabilizes the helix for about 12,000 fs as evidenced in the cluster of 3 points in the  $\alpha$ -helical region in Figure 20.

The randomization of the  $\beta$ -sheet conformation is due to the fact that MD simulations were made for isolated  $\beta$ -chains. As shown in Figure 17, the spiropyran chromophore also appears to enhance this randomization, whereas the merocyanine has little effect. The  $\beta$ -structure achieves stabilization normally from intermolecular hydrogen bonding between parallel or anti-parallel sheets. During these MD simulations on the isolated chain, the  $\beta$ -sheet conformation occasionally gains stability by the formation of intramolecular hydrogen bonds between the  $i^{\text{th}}$  and  $(i+2)^{\text{th}}$ , or  $i^{\text{th}}$  and  $(i+3)^{\text{th}}$  amino acid residues as the  $\beta$ -sheet structure randomizes. Figure 21 shows the number of H-bonds formed in the  $\beta$ -structures during the dynamics.

The extent of helical backbone distortion depends on the attachment site on the chromophore. The fluctuations in the peptide chain attached to the indoline and benzopyran groups of the chromophore are slightly different. Table 5 shows the statistical analysis of the end-to-end distance of the chains attached to either

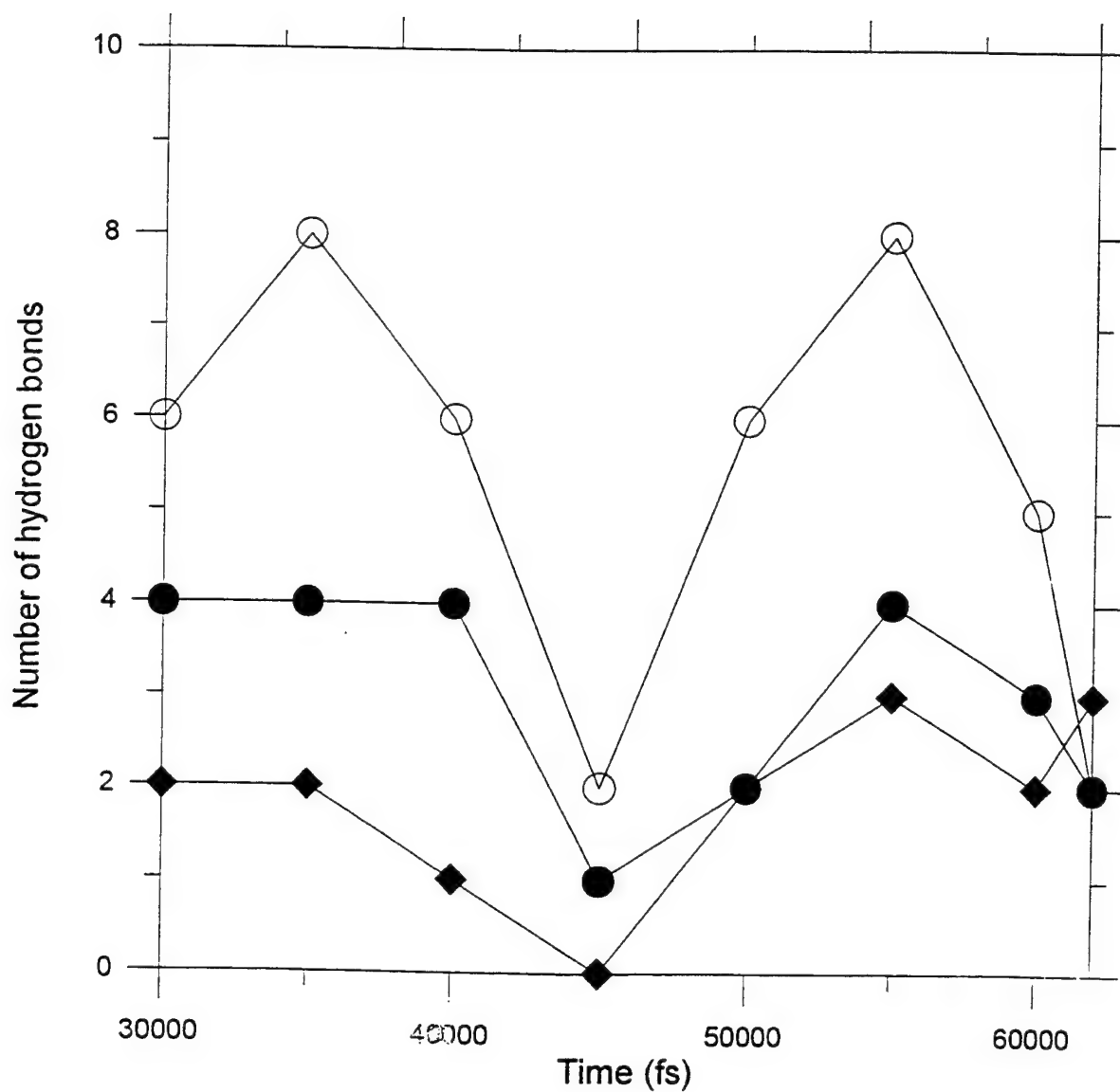


Figure 18. Number of H-bonds in  $\alpha$ -helical structures (both chains) during simulation [♦ = pA[ $\alpha$ ]-M-pA[ $\alpha$ ], • = pA[ $\alpha$ ]-S-pA[ $\alpha$ ], O = pA[ $\alpha$ ]

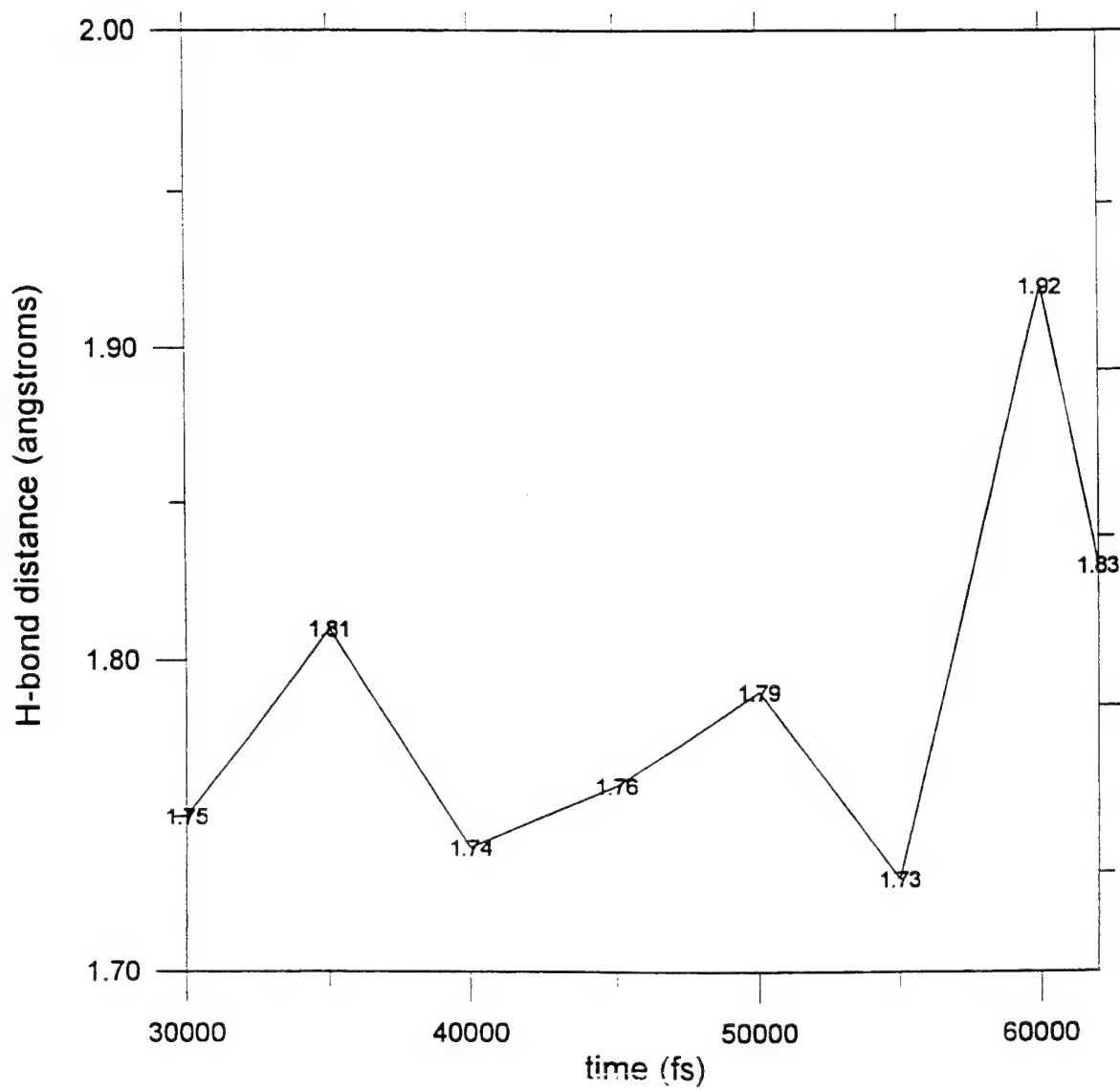


Figure 19. Variation in distance of H-bond ( O---H ) in pA[α]-M-pA[α]

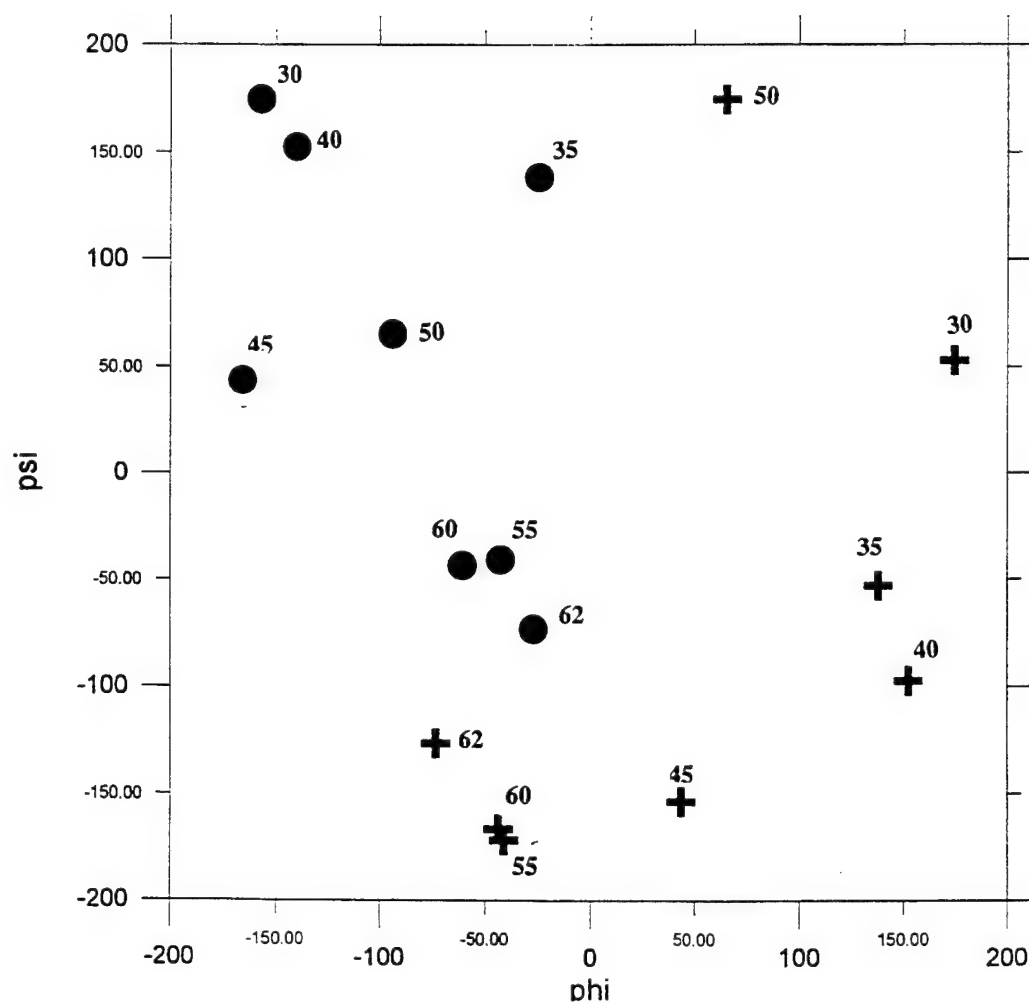


Figure 20. Conformation of alanine residues attached to the indoline and benzopyran groups of merocyanine. ( + = ala 1 at indoline side, • = ala 1 at benzopyran side; numbers by the points indicate the time step )

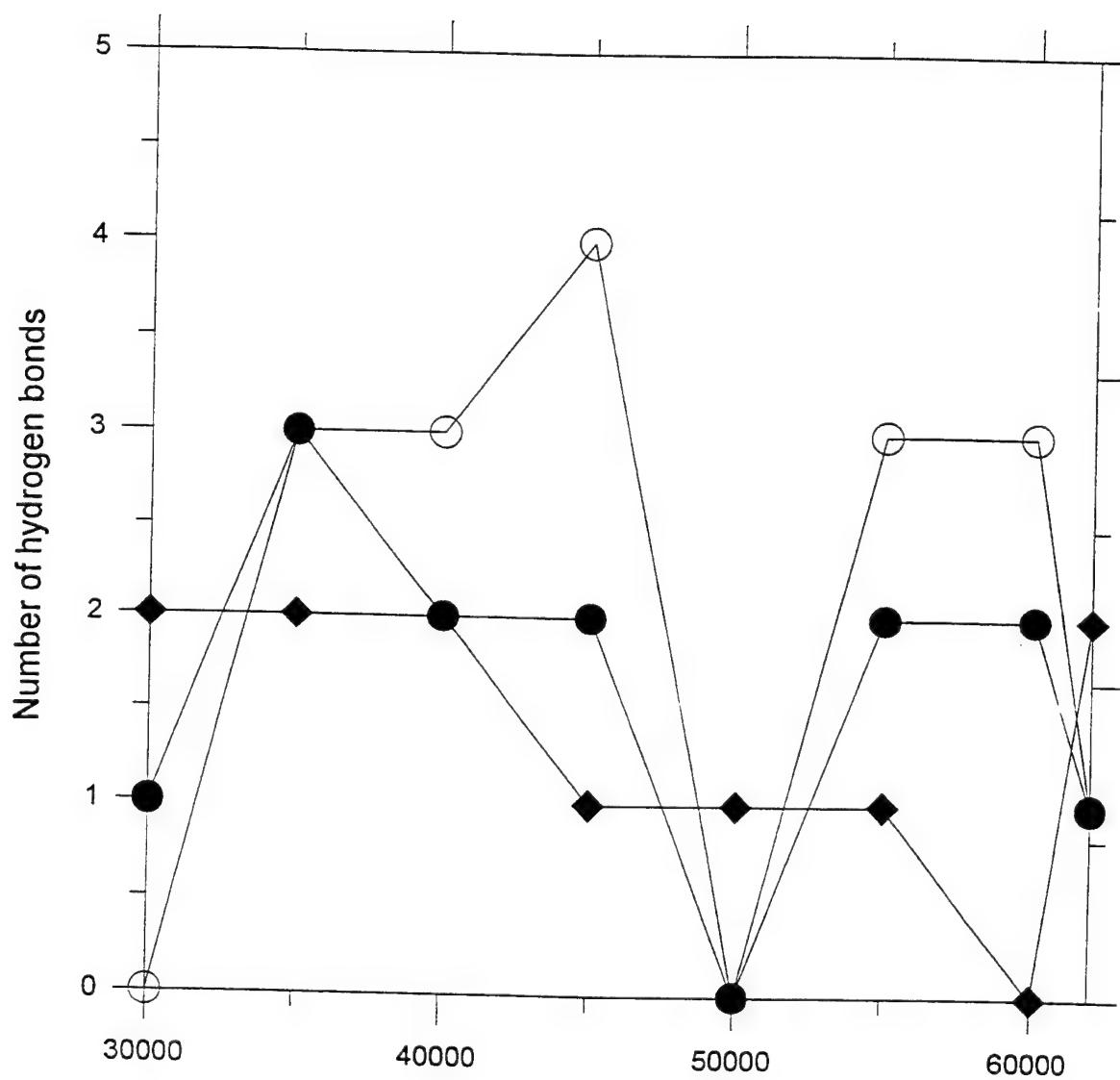


Fig. 21. Number of H-bonds in  $\beta$ -structures during simulation

[ $\diamond$  = pA[ $\beta$ ]-M-pA[ $\beta$ ],  $\bullet$  = pA[ $\beta$ ]-S-pA[ $\beta$ ],  $\circ$  = pA[ $\beta$ ]

side of the chromophore. Standard deviations of 2.7 Å and 2.3 Å are observed for the chains attached to the indoline and benzopyran groups of merocyanine, respectively. Because the average end-to-end distance is closer to the initial length of the helix, the chain attached to the benzopyran group shows relatively more helical character. A similar result was found for the benzothiazoline spiropyran with attached  $\alpha$ -helical chains. The situation is reversed in the closed spiropyran-biopolymer systems. The fluctuations in the end-to-end distance are higher at the benzopyran ring, as shown in Table 5.

Figures 22 and 23 show the molecular conformations of the polypeptide-chromophore systems at 5,000 fs intervals between 30,000 and 60,000 fs. The starting model is shown at the upper left-hand corner while the other seven conformations are at 30,000 to 60,000 fs ( in intervals of 5000 fs ) with time increasing left to right and top to bottom. The hydrogen bonds are shown by dashed lines. The sidechains have been omitted for the sake of clarity. The starting and ending conformations of  $\alpha$ -helical and  $\beta$ -poly-L-alanine spiropyran systems and unsubstituted poly-L-alanine are shown in Figure 24.

From the end-to-end distance analysis, it can be speculated that after the chromophore absorbs UV light to form the merocyanine, reversion to the initial closed form may be retarded. Although no experimental evidence of this irreversibility is available, the fact that the merocyanine-bound poly-L-alanine system assumes a more helical character for the attached polypeptide chain indicates that it is more stable than the spiropyran-poly-L-alanine system. The spiropyran-biopolymer structure ( with reduced helical character) exists as a more compact structure, hence, is expected to be less stable than the merocyanine analog. Thus, the packing of the poly-L-alanine segments may substantially alter the ability of the spiropyran to open and close, affecting its sensitivity to UV radiation and the kinetics of the color change.

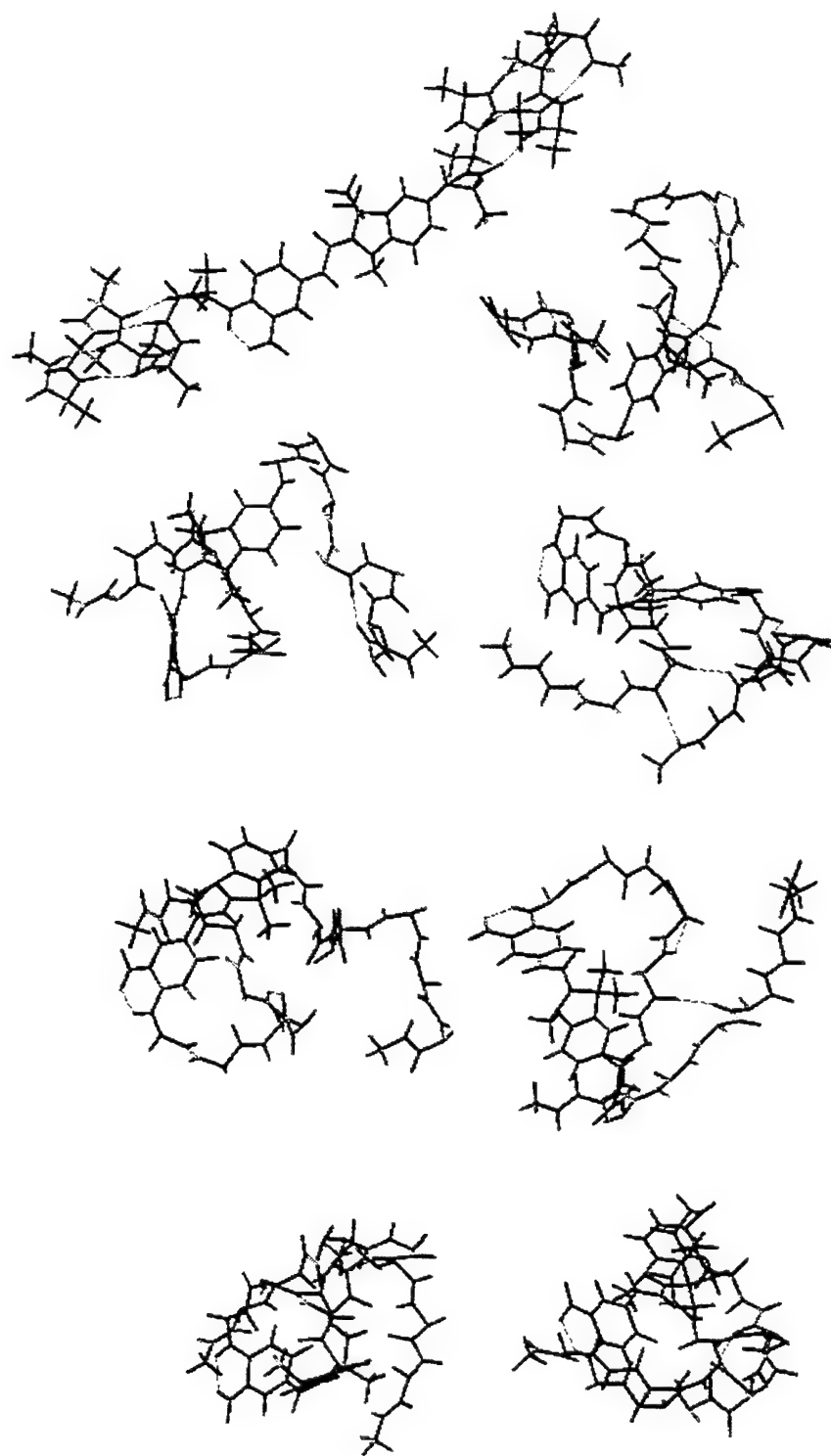


Fig. 22. Molecular motions of pA[ $\alpha$ ]-M-pA[ $\alpha$ ]

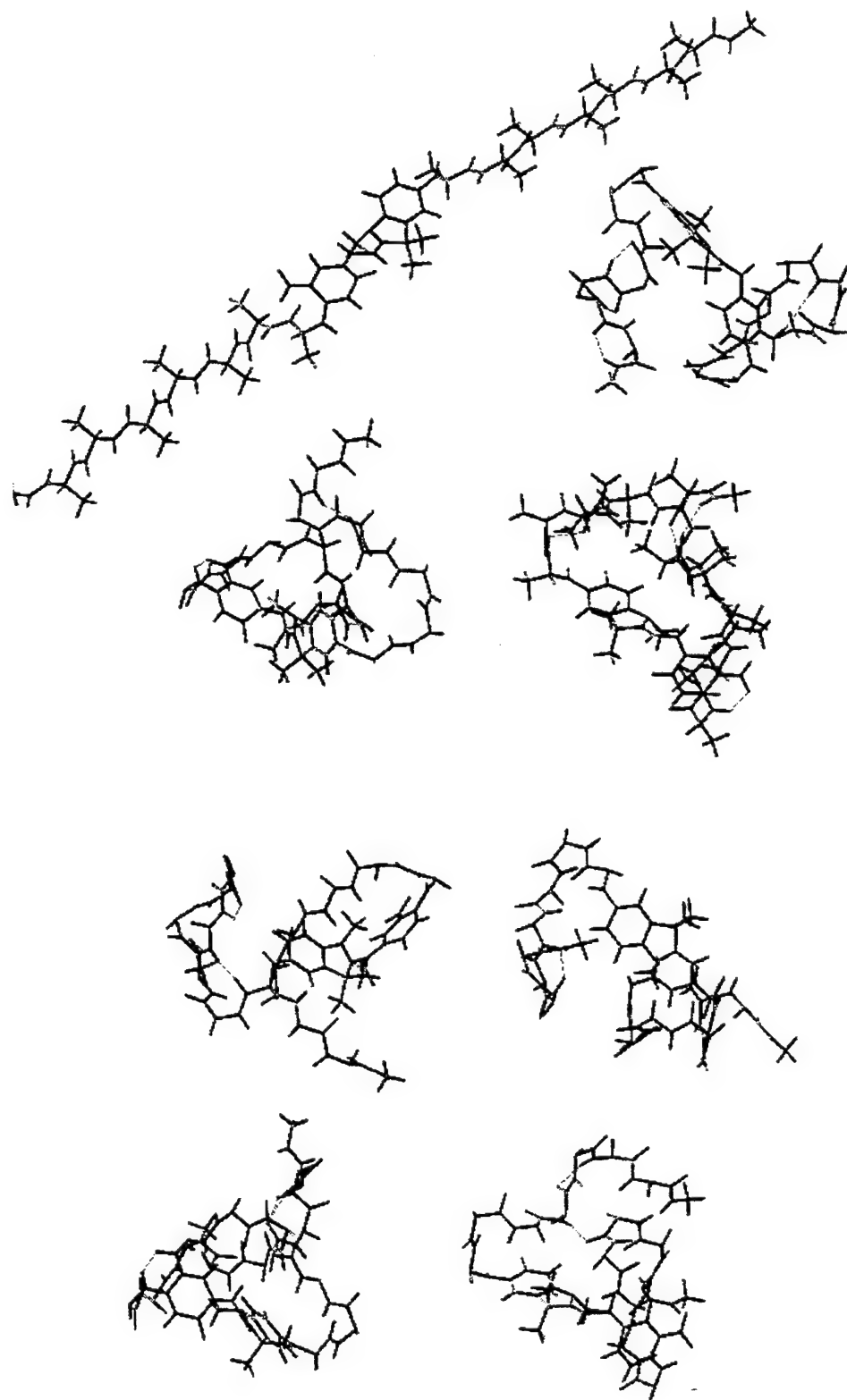
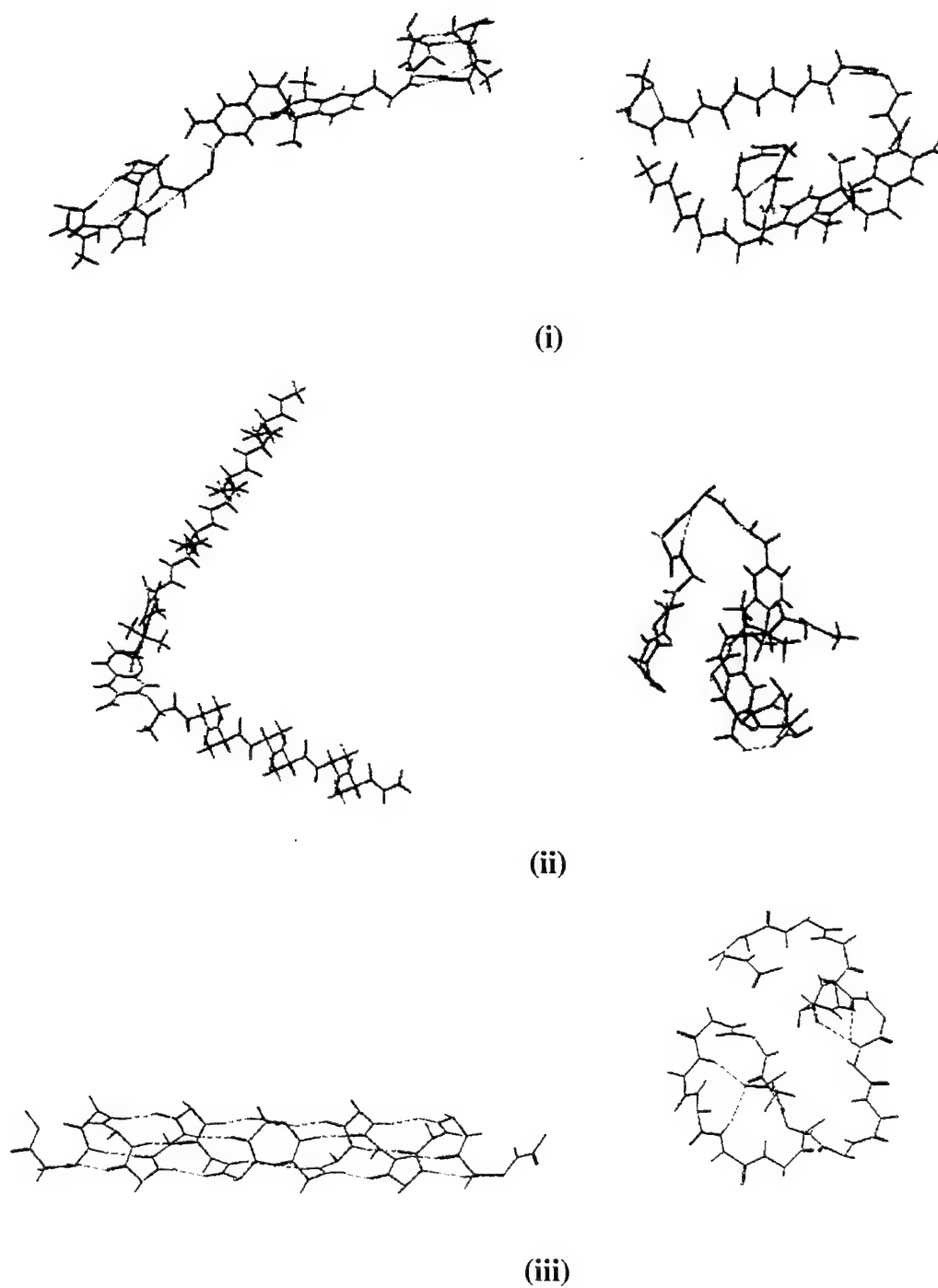


Fig. 23. Molecular motions of pA[β]-M-pA[β]





**Fig. 24.** Molecular motions of (i) pA[ $\alpha$ ]-S-pA[ $\alpha$ ], (ii) pA[ $\beta$ ]-S-pA[ $\beta$ ], and (iii) pA[ $\alpha$ ]

### 3.3.2. Chromophore-Copolymer Systems

Shown in Tables 7 and 8 are the statistics of the end-to-end distance of two types of copolymer chains attached to the chromophore. The values on the left are for the chains attached to the indoline side, while those on the right are for the chains on the benzopyran side. As was done previously, the value presented in the table is for the first 7 of the 20 residues in the unsubstituted copolymer. As found for unsubstituted poly-L-alanine, the unsubstituted copolymer chain shows the smallest deviation, indicating that the presence of the chromophore generally causes increased distortion of the biopolymer chain. For the  $\alpha$ -helical septipeptide, the merocyanine-substituted form shows an average distance close to the initial value of the helix. As observed for the homopolymer chains, the spiropyran causes the copolymer chains, initially in either the  $\alpha$ -helical or  $\beta$ -sheet conformation to assume more compact structures, while the merocyanine leads to larger end-to-end distances than for the unsubstituted copolymer.

Table 7. Statistical analysis of end-to-end distance of  $\alpha$ -poly(asp-arg-leu-ala-ser-tyr-leu) ( Co-II[ $\alpha$ ] ) chains attached to indoline chromophore and in the unsubstituted form.

initial length of helix = 11.0 Å

	Co-II[ $\alpha$ ]-M-Co-II[ $\alpha$ ]	Co-II[ $\alpha$ ]-S-Co-II[ $\alpha$ ]	Co-II[ $\alpha$ ]
average (Å)	12.0, 9.4	5.6, 11.5	12.0
Std deviation (Å)	1.6, 1.33	1.1, 1.0	0.3

Table 8. Statistical analysis of end-to-end distance of  $\beta$ -poly(gly-ser-gly-ala-gly-ala) ( Co-I[ $\beta$ ] ) chains attached to indoline chromophore and in the unsubstituted form.

initial length of  $\beta$ -chain = 20.0 Å

	Co-I[ $\beta$ ]-M-Co-I[ $\beta$ ]	Co-I[ $\beta$ ]-S-Co-I[ $\beta$ ]	Co-I[ $\beta$ ]
average (Å)	14.0, 11.2	6.9, 9.20	10.4
Std deviation (Å)	2.0, 2.6	1.6, 1.4	0.6

The homopolymer-chromophore systems show a higher deviation in the end-to-end distance of the chains than the copolymer-chromophore systems. As observed for the homopolymer case, the extent of distortion of the biopolymer chain depends on the site of attachment of the chain. The merocyanine results in more extended structures and the spiropyran results in more collapse for the polypeptide attached to the indoline ring of the chromophore. Comparison with the homopolymer-chromophore systems shows that the effect of the chromophore on the biopolymer chains depends more on the starting conformation of the biopolymer than on the specific amino acid sequence. The additional stabilization effect from the hydrogen bond ( formed between the oxygen in the NO<sub>2</sub> on the merocyanine and the amide proton of the first residue ) is minimal in the copolymer-chromophore system as this bond, even though formed initially, is broken during the simulation.

### 3.3.3. Variation in the $\phi$ and $\psi$ Dihedral Angles

Shown in Tables 9 and 10 are the averages of the internal coordinates,  $\phi$  and  $\psi$ , of the seven alanine residues in the  $\alpha$ - and  $\beta$ -chains attached to the indoline ring of the chromophore ( from 30,000 fs to 31,000 fs of simulation ). Figures 25 and 26 show the  $\phi$ ,  $\psi$  plot for each alanine residue starting in the  $\alpha$ -helical and  $\beta$ -conformations respectively. Both show large excursions of the dihedral angles from their initial values, suggesting a randomization of these conformations.

Table 9. Average values of the internal coordinates,  $\phi$  and  $\psi$ , in an  $\alpha$ -helical chain of poly-L-alanine-merocyanine system

residue #	1	2	3	4	5	6	7
$\phi$ $-58^\circ$	-152( 8.0)	-77(8.0 )	-127(21.0 )	-71( 22.0)	-96(19.0 )	-140(12.0 )	-161(22.0 )
$\psi$ $-47^\circ$	120( 7.0)	-51(13.0 )	52( 8.0)	161(6.0 )	-68( 19.0)	61(22.0 )	117(17.0)

[Numbers in parenthesis show standard deviation]

Table 10. Average values of the internal coordinates,  $\phi$  and  $\psi$ , in a  $\beta$  chain of poly-L-alanine-merocyanine system

residue #	1	2	3	4	5	6	7
$\phi$ $-139^\circ$	-92(6.0)	50(11.0)	76(16.0)	-104(11.0)	-79(16.7)	-105(34.5)	-116(34.0)
$\psi$ $135^\circ$	162(11.0)	65(7.0)	112(11.0)	46(11.0)	-50(11.6)	59(20.3)	79(26.7)

[Numbers in parenthesis show standard deviation]

To gain insight into the progression of helical character along the peptide backbone, a  $\phi$ ,  $\psi$  plot for the merocyanine-substituted- $\alpha$ -poly-L-alanine is constructed for alanine residues 1, 4 and 7. Figure 27 shows the  $\psi$ ,  $\phi$  values after every 5,000 fs. The  $\phi$ ,  $\psi$  values of alanine residue 1 are close to the ideal values for an  $\alpha$ -helix. (  $-47^\circ$ ,  $-58^\circ$  respectively ) for about 12,000 fs of the simulation. This results from the stabilization effect of the hydrogen bond which is formed between the oxygen in  $\text{NO}_2$  of the merocyanine and the amide proton of the alanine residue.

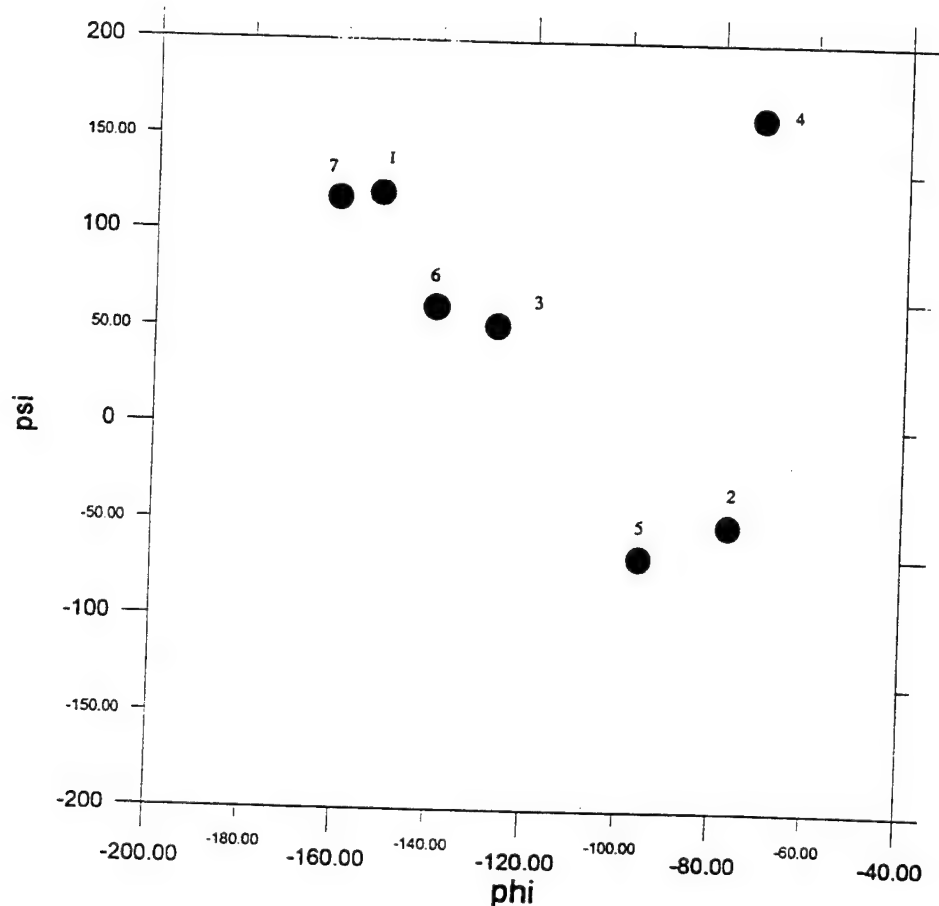


Fig. 25. Average  $\phi$  and  $\psi$  dihedral angles of  $\alpha$ -helical alanine residues ( numbers indicate residue number )

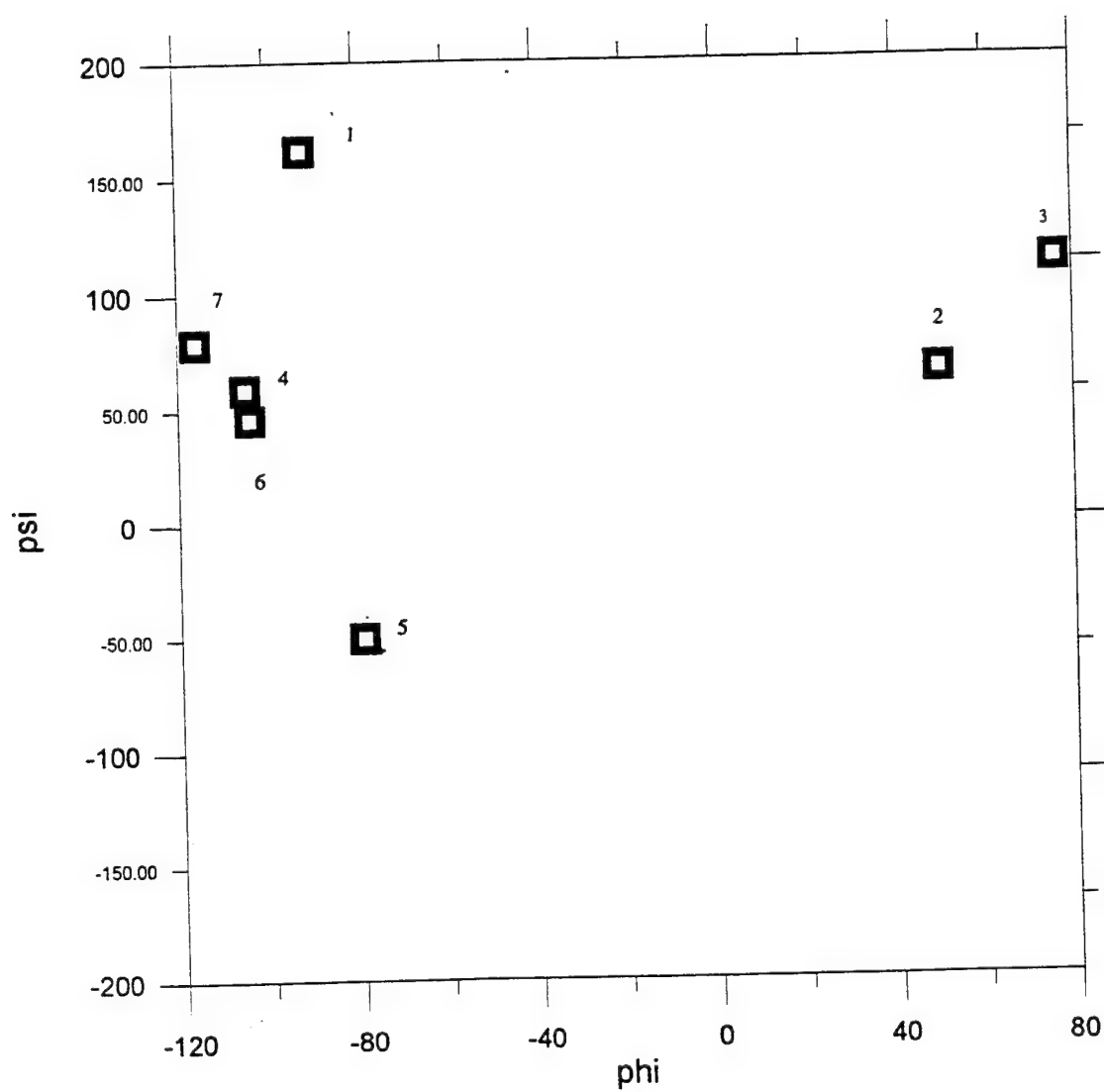


Fig. 26. Average  $\phi$  and  $\psi$  dihedral angles of  $\beta$ -alanine residues (numbers indicate the residue number)

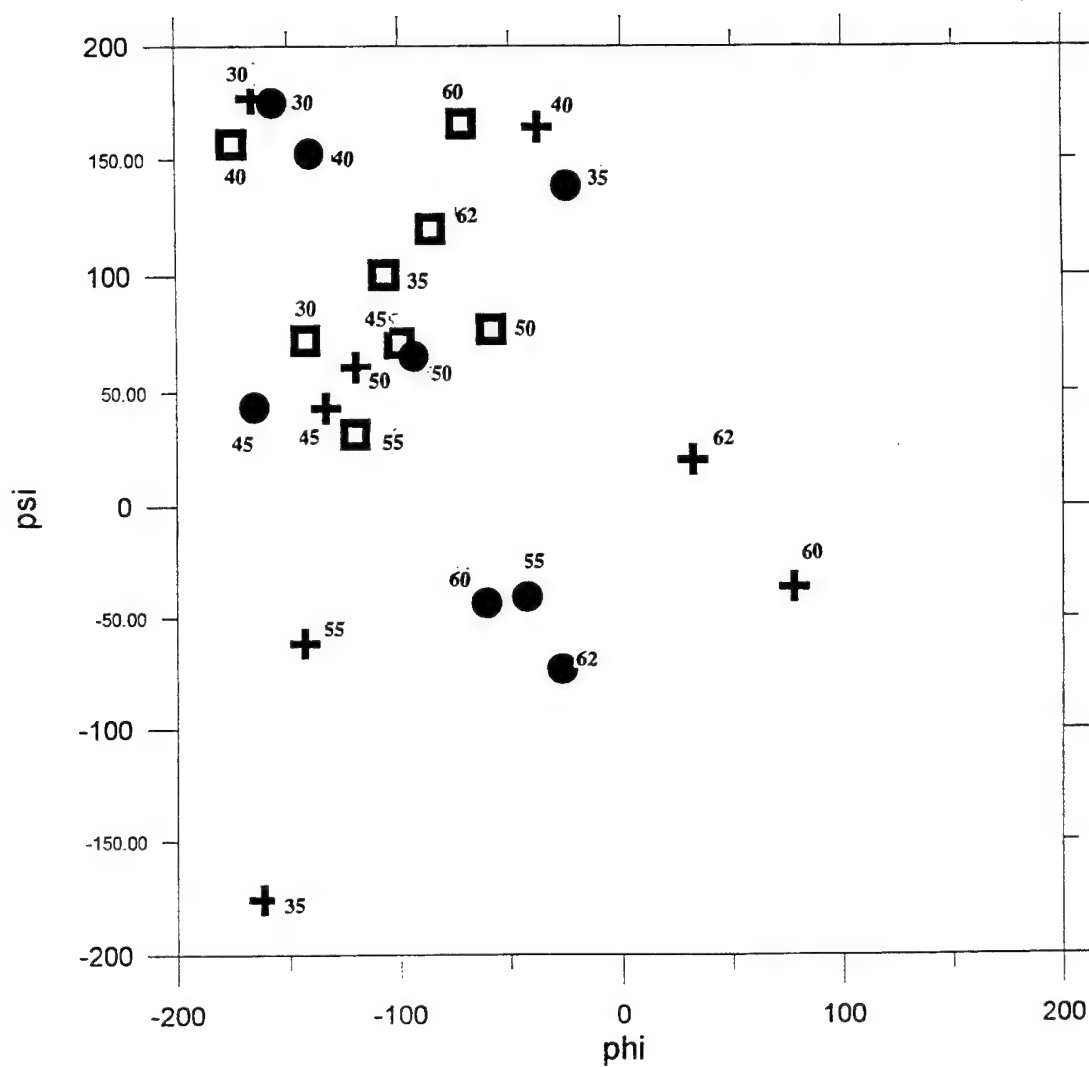


Fig. 27.  $\phi / \psi$  variations in alanine residues 1, 4, and 7. (pA[ $\alpha$ ]-M-pA[ $\alpha$ ])  
 (• = residue 1, + = residue 4,  $\square$  = residue 7; numbers indicate time step )

### 3.4. Molecular Dynamics of Benzothiazoline-spiro-benzopyran-poly-L-alanine Systems

Tables 11 and 12 show the end-to-end distance fluctuations in the biopolymer chains attached to the benzothiazoline spiropyran. As observed for the indoline spiropyran-biopolymer systems, the extent of chain distortion depends on the attachment site on the chromophore. The  $\beta$ -sheet conformation is

Table 11. Statistical analysis of end-to-end distances of  $\alpha$ -poly-L-alanine attached to benzothiazoline spiropyran ( BZM/BZS ). (Values on the left are for the chains attached to the thiazoline group, while those on the right are for the chains attached to the benzopyran group.)

initial length of helix = 11 Å

	pA[ $\alpha$ ]-BZM-pA[ $\alpha$ ]	pA[ $\alpha$ ]-BZS-pA[ $\alpha$ ]
average (Å)	11.4, 16.2	12.1, 12.0
Std deviation (Å)	3.2, 3.1	2.0, 3.7

Table 12. Statistical analysis of end-to-end distance of  $\beta$ -poly-L-alanine attached to benzothiazoline spiropyran ( BZM/BZS ).

initial length of  $\beta$ -chain = 24.0 Å

	pA[ $\beta$ ]-BZM-pA[ $\beta$ ]	pA[ $\beta$ ]-BZS-pA[ $\beta$ ]
average (Å)	12.6, 12.0	9.1, 7.0
Std deviation (Å)	4.0, 3.7	2.7, 1.5



destabilized more than the  $\alpha$ -helix. This result is consistent with that obtained for the peptide-indoline spiropyran system. The hydrogen bond which is formed between the oxygen in the  $\text{NO}_2$  in the merocyanine form of indoline spiropyran is absent initially in the benzothiazoline-biopolymer system. The bond forms as the MD simulation progresses, thus stabilizing the biopolymer chain to some extent. The values for the spiropyran and merocyanine are more similar than in the indoline spiropyran-biopolymer systems. This may be due to the fact that the additional stability gained by the merocyanine ( from the hydrogen bond ) is less than in the indoline-type systems. Figure 28 shows the end-to-end distance plots for  $\alpha$ -helical poly-L-alanine chain attached to the thiazoline ring of the benzothiazoline spiropyran chromophore, while Figure 29 shows a similar plot for  $\beta$ -poly-L-alanine. The closed chromophore- $\beta$ -sheet structure randomizes into a more compact structure as observed for the indoline spiropyran-biopolymer systems. The  $\beta$ -sheet shows a tendency to assume a helical conformation by forming  $i^{\text{th}}-(i+2)^{\text{th}}$  hydrogen bonds during the simulation, as also observed for the indoline spiropyran systems. However, the number of hydrogen bonds formed is fewer than in the indoline spiropyran systems as shown in Figure 30. Shown in Figures 31 and 32 are the molecular conformations of the poly-L-alanine-benzothiazoline spiropyran systems after every 5,000 fs simulation. The starting structures for the  $\alpha$ -helical and  $\beta$ -poly-L-alanine systems are shown at the top left. The time of the figures increases from left to right and top to bottom. The starting and ending conformations of  $\alpha$ -helical and  $\beta$ -poly-L-alanine-benzothiazoline-spiropyran systems are shown in Figure 33.

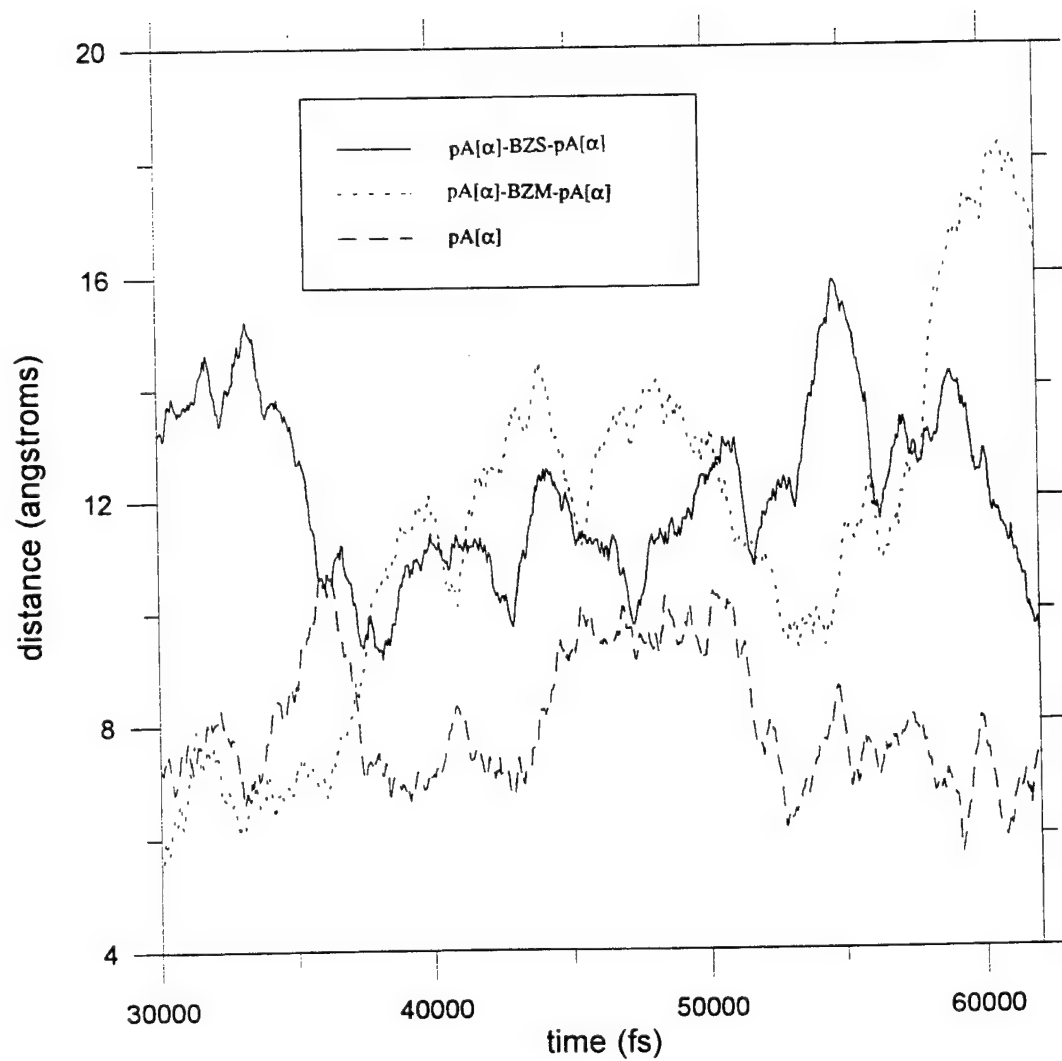


Fig. 28. End-to-end distance as a function of time

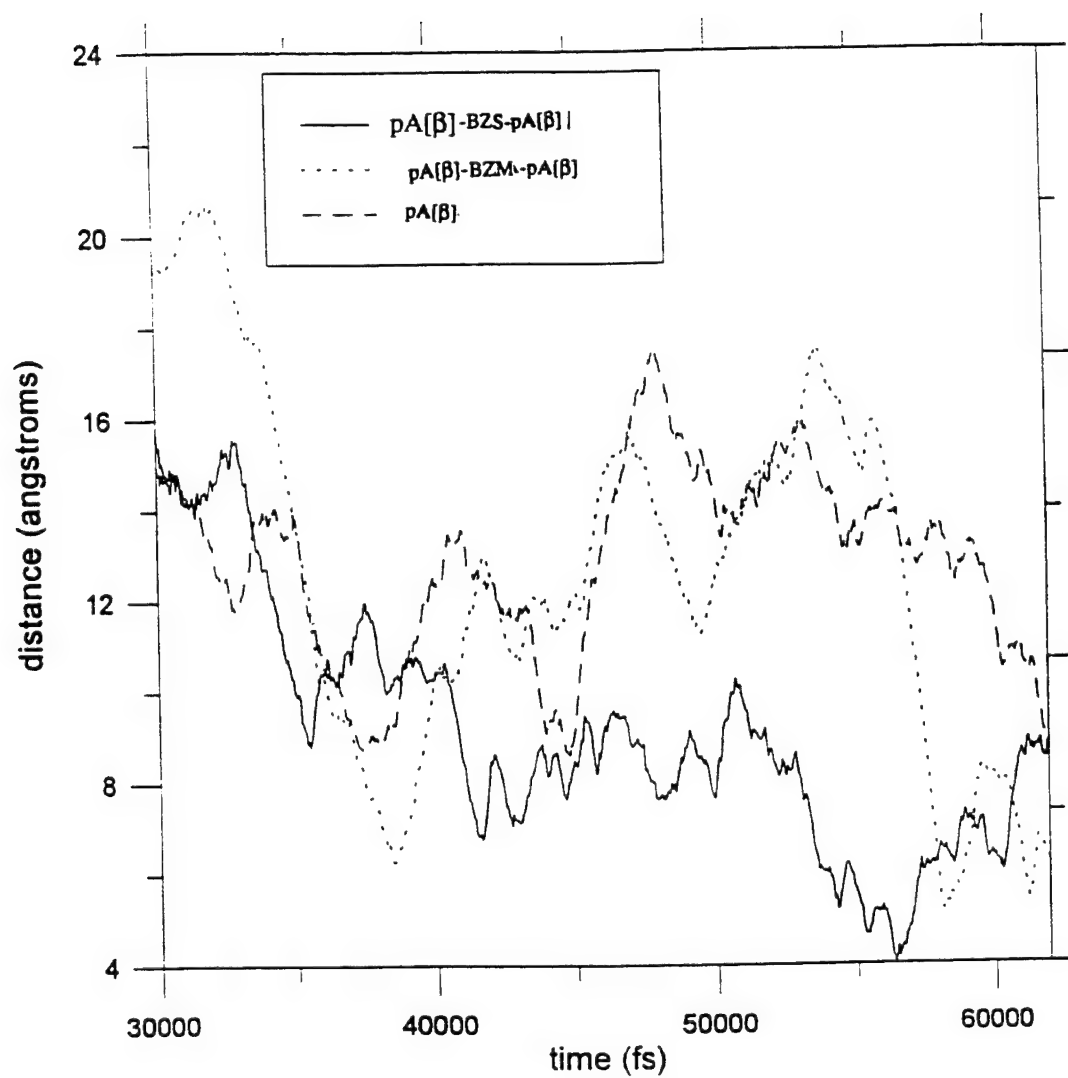


Fig. 29. End-to-end distance as a function of time

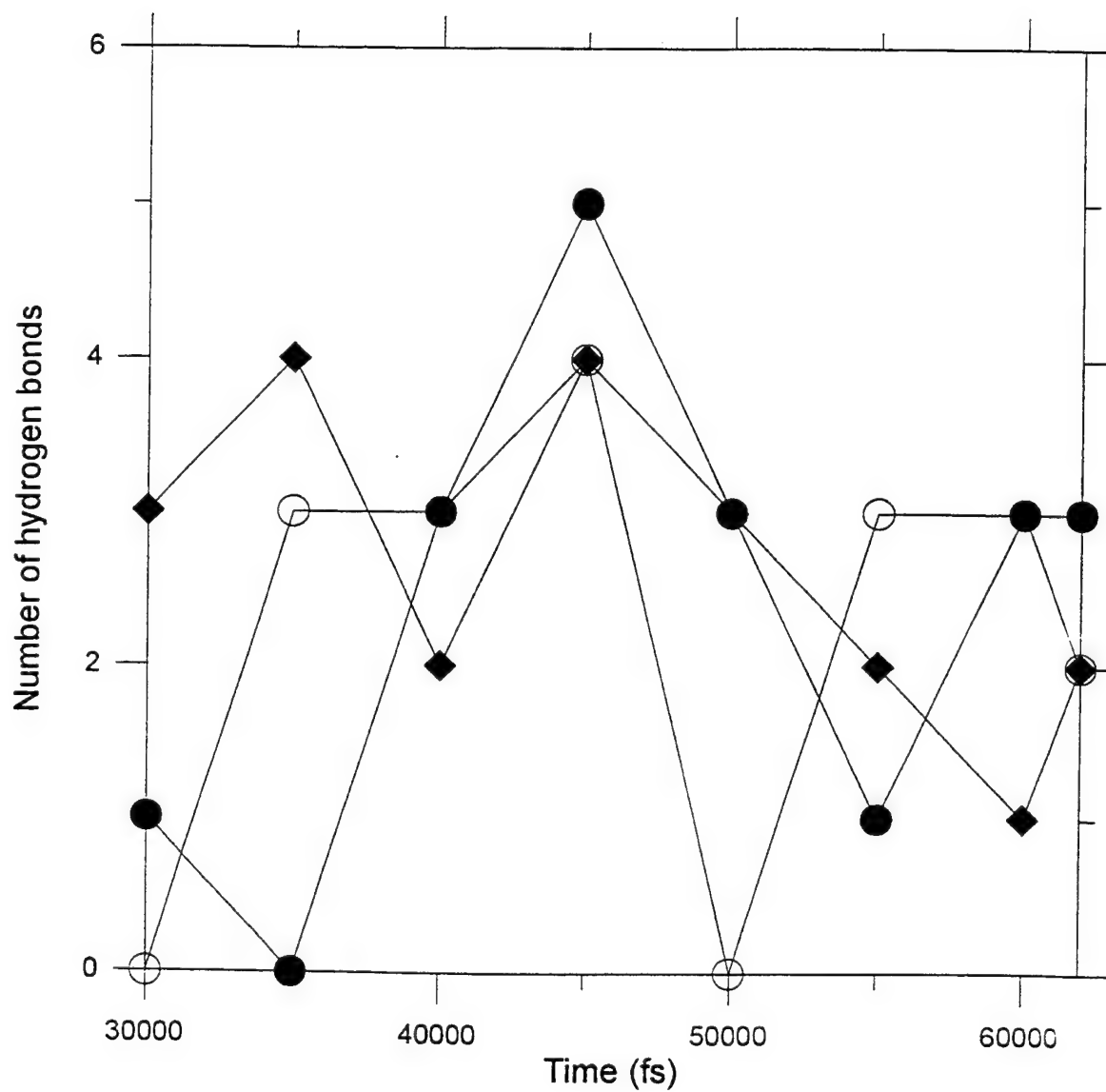


Fig. 30. Number of H-bonds formed in the  $\beta$ -structures (both chains) during simulation. [♦ = pA[ $\beta$ ]-BZM-pA[ $\beta$ ], • = pA[ $\beta$ ]-BZS-pA[ $\beta$ ], O = pA[ $\beta$ ]

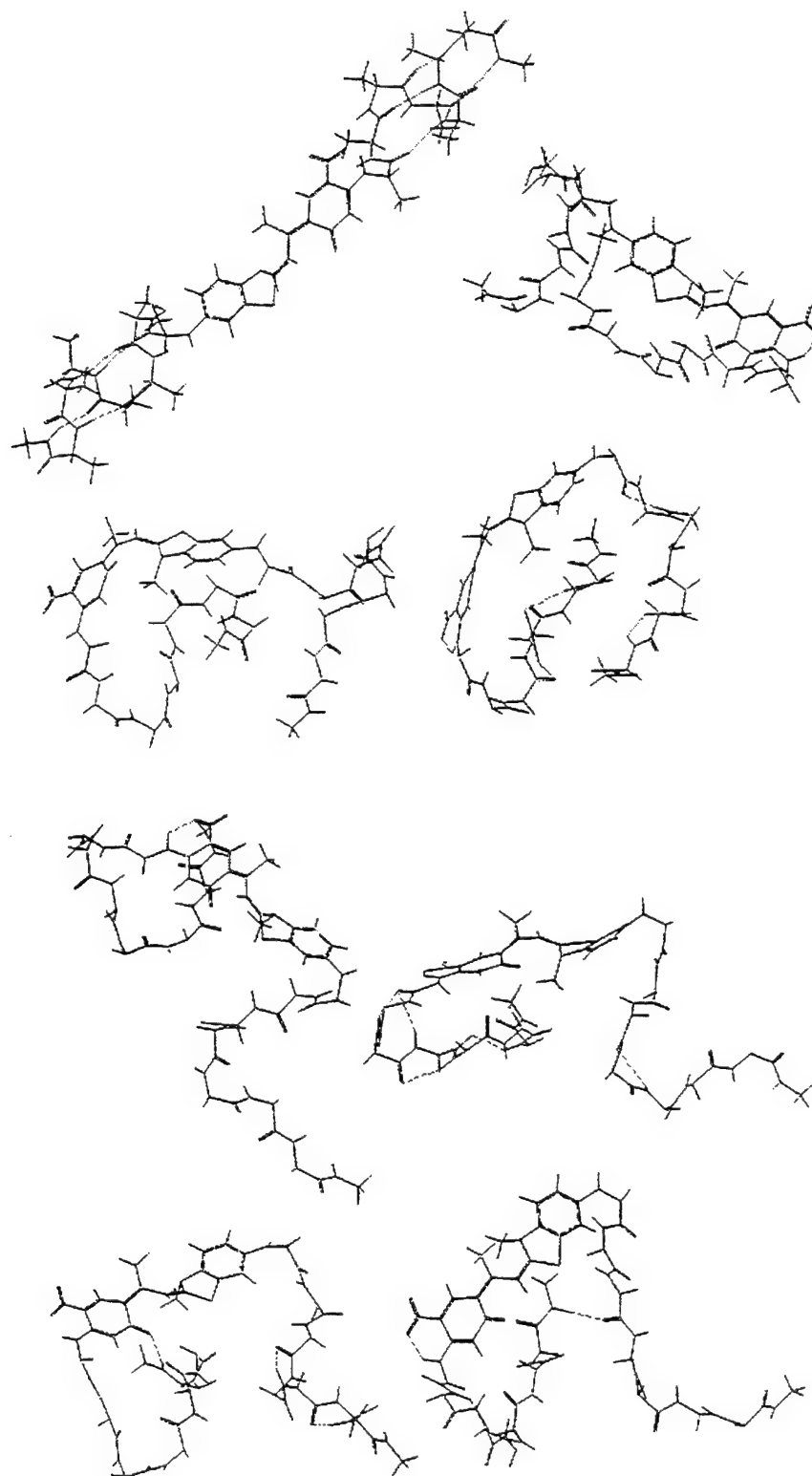
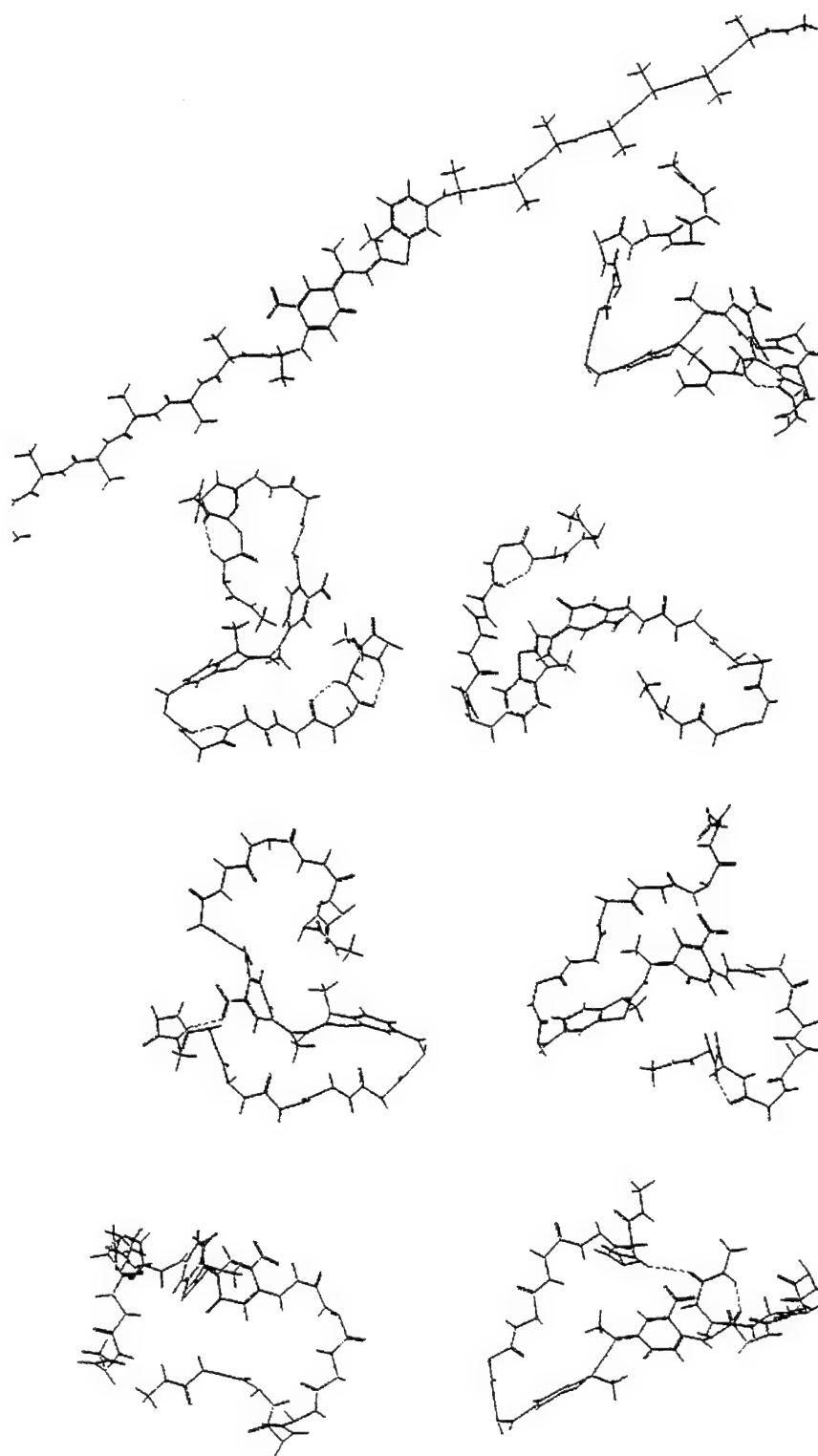
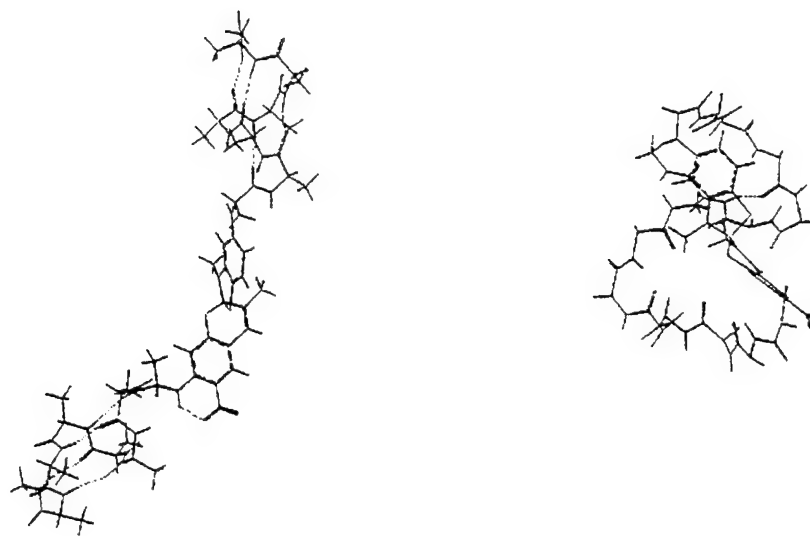


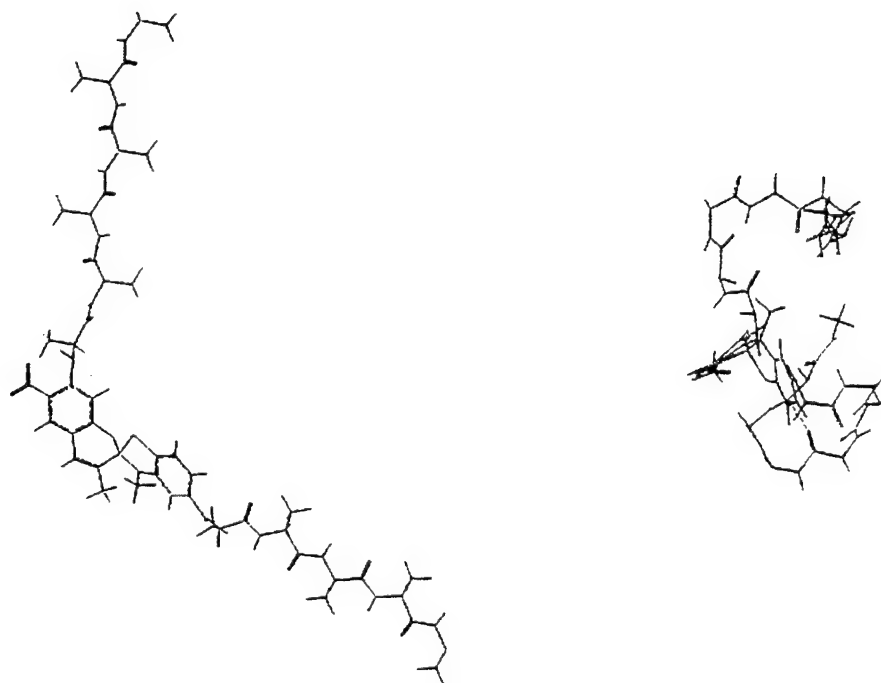
Fig. 31. Molecular motions of pA[ $\alpha$ ]-BZM-pA[ $\alpha$ ] after every 5,000 fs



**Fig. 32.** Molecular motions of pA[β]-BZM-pA[β] after every 5,000 fs



(i)



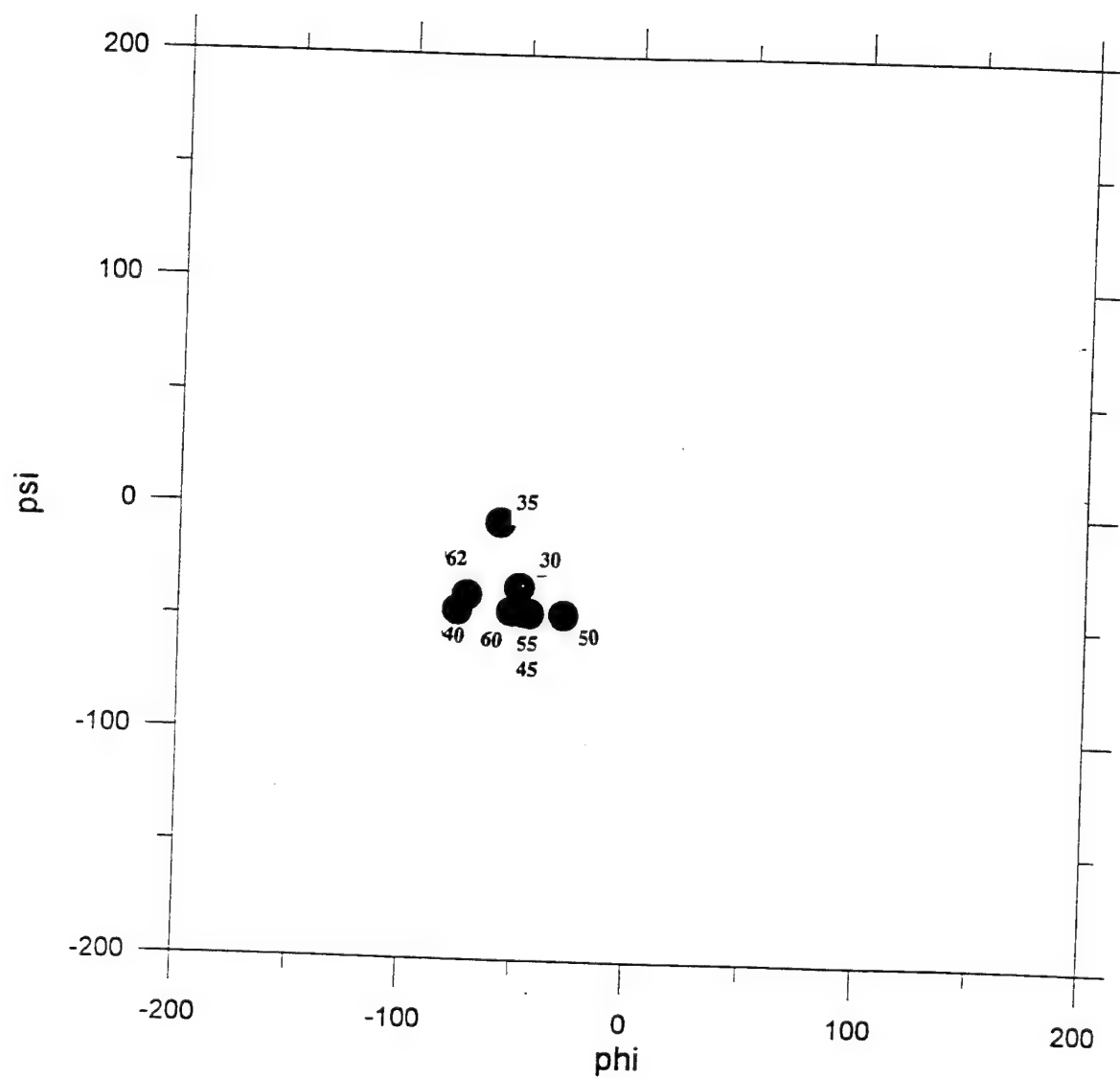
(ii)

Fig. 33. Molecular motions of (i)  $\text{pA}[\alpha]\text{-IBZS[-pA}[\alpha]$ , (ii)  $\text{pA}[\beta]\text{-BZS-pA}[\beta]$

### 3.4.1. Variation in $\phi$ and $\psi$ Dihedral Angles

Figure 34 shows the molecular conformations of the first alanine residue of unsubstituted poly-L-alanine during the dynamics. Results from similar  $\phi, \psi$  plots for the benzothiazoline and indoline spiropyran-poly-L-alanine systems show that both variations of the spiropyrans cause a significant deviation in the internal coordinates of the biopolymer chains (from the ideal  $\phi, \psi$  values of  $-58^\circ$  and  $-47^\circ$ , respectively) during the MD simulation. This implies that the presence of the chromophore causes the ordered  $\alpha$ -helical and  $\beta$ -sheet conformations to change into a random conformation. Comparison of Figure 20 with the  $\phi, \psi$  plot in Figure 35 for the first alanine residues in the polypeptide chain shows that the stabilization effect of the hydrogen bond on the conformation is less than observed in the indoline spiropyran-biopolymer system. The internal coordinates  $\phi, \psi$  remain close to the ideal  $\alpha$ -helical values for only 5,000 fs, as compared to 12,000 fs in the indoline spiropyran-biopolymer systems. This is due to the fact that the hydrogen bond is formed occasionally during the dynamics as the distance between the oxygen atom and the amide proton gets closer to  $\sim 1.8 \text{ \AA}$  ( the ideal value for an O-H bond distance ). The diminished steric effect in the benzothiazoline chromophore structure, as a result of the absence of the 3'-methyl substituents, reduces the fluctuations in the chain attached to the thiazoline ring as compared to the indoline ring ( of the indoline chromophore ).





**Fig. 34. Molecular conformation of ala1 of pA[α]**  
(numbers by the points indicate the time step)

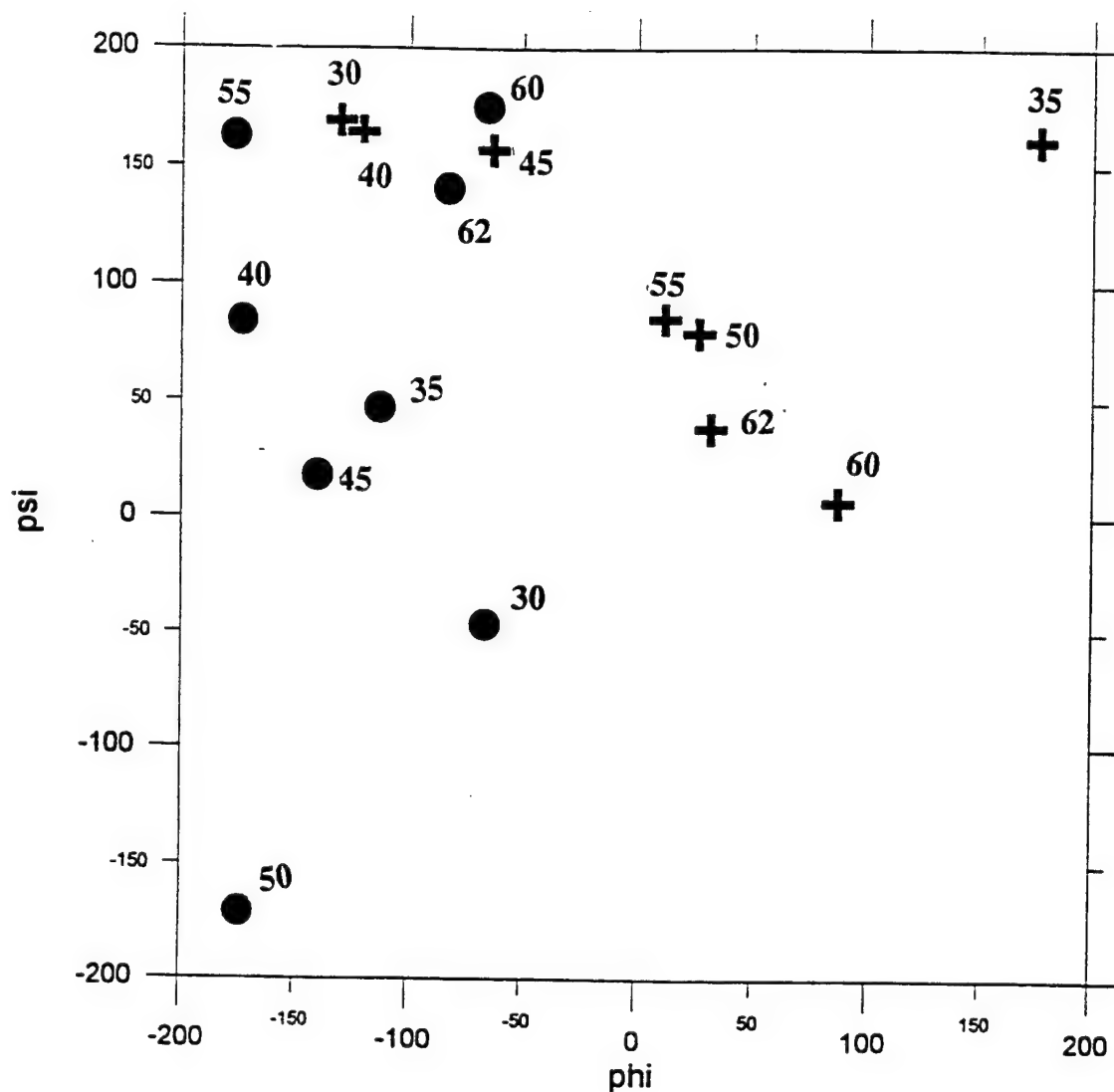


Figure 35. Molecular conformations of alanine residues attached to the benzothiazoline and benzopyran groups of pA[ $\alpha$ ]-BZM-pA[ $\alpha$ ]. ( + = ala 1 on indoline side, • = ala 1 on pyran side; numbers by the points indicate the time step )

## Section 4

### CONCLUSIONS

Computational chemistry methods have been used to explore the properties of poly-L-alanine-spiropyran and copolymer-spiropyran systems. An understanding of the molecular structure of these photochromic biopolymer systems helps in achieving high  $\chi(2)$  or  $\chi(3)$  nonlinear optical properties. Molecular mechanics was used to generate and evaluate conformations for the chromophore-biopolymer system. Results on the energetics of both poly-L-alanine and the copolymer systems indicate that an increase in energy of about 16 to 30 kcal/mol occurs when the indoline or benzothiazoline form of the spiropyran chromophore is coupled to  $\beta$ - or  $\alpha$ -poly-L-alanine. The large difference in energy between the unsubstituted  $\alpha$ -helical poly-L-alanine and poly-L-alanine in the  $\beta$ -sheet conformation is due to the fact that the calculations were done on an isolated chain of  $\beta$ -poly-L-alanine in which the stabilization effect of intermolecular hydrogen bonding is absent. Molecular dynamics simulations give insight into the effects of the chromophore on the conformational properties of the polypeptide and the inherent flexibility in the chromophore-biopolymer system. Statistical analysis of the end-to-end distance during the simulations shows that the merocyanine results in more extended structures and the spiropyran results in more collapse for the polypeptide attached to the indoline ring of the chromophore. The hydrogen bond which is formed between the oxygen (in the  $\text{NO}_2$  group) in the merocyanine chromophore and the amide proton of the first alanine residue in the peptide chain stabilizes the  $\alpha$ -helix to some extent. The  $\beta$ -sheet structures achieve

stability by forming intramolecular hydrogen bonds between the  $i^{\text{th}}$  and the  $(i+2)^{\text{th}}$ , or  $i^{\text{th}}$  and  $(i+3)^{\text{th}}$  amino acid residues.

The effect of the chromophore on the biopolymer chains depends more on the starting conformation of the biopolymer than on the specific amino acid sequence.

## Section 5

### FUTURE WORK

Future work should be carried out using semiempirical molecular orbital calculations to explore the photochemical processes, electron distributions as a function of substituents and conformation, and electronic interactions between the biopolymer and chromophore.

The molecular packing and intermolecular interactions should be analyzed in relation to molecular structure. Large layered assemblies of molecules should be studied to examine end-group packing and to provide adequate boundary conditions for the models.

These analyses would serve as a useful tool for further prediction of experimental properties.

## Section 6

### REFERENCES

- ( 1 ) Vandewyer, P.H., Smets, G., J. Polym. Sci., 1970, **8**, pp. 2364-2374.
- ( 2 ) Cooper, T.M., Obermeier, K.A., Crane, R.L., Photochem.& Photobiol., 1992, **55**, pp. 1-7.
- ( 3 ) Suzuki, Y., Ozawa, K., Hosoki, A., Ichimura, K., Poly. Bull., 1987, **17**, pp. 285-291.
- ( 4 ) Yamamoto, H., Miyagi, Y., Nishida, A., Tagagishi, T., Shima, S., J. Photochem., **39**, 343-350.
- ( 5 ) Ueno, A., Takahashi, K., Anzai, J., Osa, T., J. Am. Chem. Soc., 1981, **103**, 5410-6415.
- ( 6 ) Ciardelli, F., Fabbri, D., Pieroni, O., Fissi, A., J. Am. Chem. Soc., 1989, **111**, pp. 3470-3472.
- ( 7 ) Pachter R., Cooper, T.M., Natarajan, Obermeier, K.A., L.V., Crane, R.L., Adams, W.W., Biopolymers, 1992, **32**, pp. 1129-1140.
- ( 8 ) Guglielmetti, R., "4n + 2 systems: spiropyrans," Review of Photochromism, by Bertelson, p. 314.
- ( 9 ) Robillard, J., Caulfield, H.J., Industrial applications of Holography, Oxford University Press, 1990, p. 151.
- ( 10 ) Bamford, C.H., Brown, L., Elliott, A., Hanby, W.E., Trotter, I.F., Proc. Roy. Soc., 1953, **B141**, p. 49.
- ( 11 ) Bamford, C.H., Elliott, A., Hanby, W.E., Synthetic Polypeptides, Academic Press, NY, 1956.
- ( 12 ) Lombardi, S.J., Fossey, S.A., Kaplan, D.K., Proceedings of the American Society for Composites - Fifth Technical Conference, 1991.

- ( 13 ) Denura, M., Asakura, T., Biotech. and Bioeng., 1989, **33**, p. 598.
- ( 14 ) McGrath, K.P., Fournier, M. J., Mason, T.L., Tirrel, D.A., J. Am. Chem. Soc., 1992, **114**, p. 727.
- ( 15 ) Walton, A.G., Blackwell, J., Carr, S.H., Biopolymers, Academic Press, New York and London, 1973, p.409.
- ( 16 ) Warwicker, J.O., J. Mol. Biol., 1960, **2**, p. 350
- ( 17 ) Lucas, F., Rudall, K.M., in Symposium on Fibrous Proteins, Edited by Crewther, W.G., Plenum, NY, 1968.
- ( 18 ) Astbury, W.T., Street, A., Phil. Trans. Roy. Soc., 1931, **A230**, p. 75.
- ( 19 ) Astbury, W.T., Woods, H.J., Phil. Trans. Roy. Soc., 1933, **A232**, p. 333.
- ( 20 ) Gray, G.W., Winsor, P.A., Liquid crystals and Plastic crystals, 1974, **1**, p. 185.
- ( 21 ) Perutz, M.F., Nature, 1951, **167**, p. 1053.
- ( 22 ) Scheraga, H.A., Nemethy, G., In Molecules in Natural Biosciences-Encomium for Linus Pauling, 1991.
- ( 23 ) Nemethy, G., Scheraga, H.A., Bull. Inst. Chem. Res. Univ. Kyoto, 1989, **66**, p. 398-408.
- ( 24 ) Lotz, B., J. Mol. Biol., 1974, **87**, p. 169.
- ( 25 ) Colonna-Cesari, F., Premilat, S., Lotz, B., J. Mol. Biol., 1974, **87**, p. 1883.
- ( 26 ) Colonna-Cesari, F., Premilat, S., Lotz, B., J. Mol. Biol., 1975, **95**, p. 71.
- ( 27 ) Pachter, R., Crane, R., Adams, W.W., in Silk Biopolymers, ACS Symposium Series 544, Edited by Kaplan, D., Adams, W.W., Farmer, B.L., Viney, C., Washington DC, 1994, p. 283-290.
- ( 28 ) Fossey, S.A., Kaplan, D., in Silk Biopolymers, ACS Symposium Series 544, Edited by Kaplan, D., Adams, W.W., Farmer, B.L., Viney, C., Washington DC, 1994, p. 270-282.
- ( 29 ) SYBYL version 6.01, Tripos Associates, Inc., St. Louis, MO.

- ( 30 ) Clark, M., Cramer, R.D. III, Opdenbosch Van, N., J. Comp. Chem., **10**, 1989, p. 982.
- ( 31 ) Buckert, Ulrich, D.C., Norman, A.L., Molecular Mechanisms ACS Monograph, 1982, **177**.
- ( 32 ) Sorensen, R. A., Liao, W.B., Boyd, R.H., Macromolecules, 1980. **13**, pp. 1178-1183.
- ( 33 ) Benedetti, E., Di Blasio, B., Pavone, V., Pedone, C., Toniolo, C., Crisma, M., Biopolymers, 1992, **32**, pp. 453-456.
- ( 34 ) Verlet, L., Phys. Rev., 1967, **159**, p. 98.
- ( 35 ) McCammon, J.A., Harvey, S.C., Dynamics of proteins and Nucleic acids, Cambridge University Press, NY, 1987.